

ADA031560

FC

(8)

# CERAMIC MATERIALS IN ROLLING CONTACT BEARINGS

## FINAL REPORT

Contract N00019-75-C-0197  
15 March 1975 to September 15, 1976

*H. R. Baumgartner*  
*G. S. Calvert*  
*P. E. Cowley*

## SUBMITTED TO

Department of the Navy  
Naval Air Systems Command  
Code AIR 52032  
Washington D.C. 20360

DDC  
RECEIVED  
NOV 4 1976  
B

Approved for public release; distribution unlimited.

NORTON COMPANY  
INDUSTRIAL CERAMICS DIVISION  
NORTON TOOL WORKS, MA. 01901

# TABLE OF CONTENTS

	PAGE
Foreword	iv
Abstract	v
Summary	vi
I INTRODUCTION	1
II BEARING DESIGN	2
III SILICON NITRIDE MATERIAL CHARACTERIZATION	5
IV BEARING FABRICATION	9
A. Roller Manufacture	9
B. Race Manufacture	12
C. Retainers	12
D. Bearing Assembly	12
V BEARING TESTING	15
A. Test Rig	15
B. Test Facility	15
C. Instrumentation	19
D. Test Procedure	19
E. Data Reduction Procedure	23
F. Test Results	26
VI POST TEST BEARING INSPECTION	33
VII CONCLUSIONS AND RECOMMENDATIONS	39
APPENDIX I	45
REFERENCES	54

ACCESSION for	
NTIS	While Section <input checked="" type="checkbox"/>
ODC	Buff Section <input type="checkbox"/>
UNANNOUNCED	<input type="checkbox"/>
JUSTIFICATION.....	
BY.....	
DISTRIBUTION/AVAILABILITY CODES	
Dist.	AVAIL. and/or SPECIAL

## LIST OF FIGURES

<u>FIGURE NUMBER</u>		<u>PAGE</u>
S1	Bearing calibration test matrix and summary of results.	viii
1	Design of test bearing KX-208.	3
2	Detail of silicon nitride roller geometry.	4
3	Strength qualification data for silicon nitride roller stock.	5
4	Rolling contact fatigue test machines.	7
5	Finish characteristics of silicon nitride RCF specimens.	8
6	Fatigue life results for silicon nitride Billet #438756 at 800 ksi stress	8
7	Roller blank dimensions.	10
8	Crowned roller dimensions.	11
9	Outer race dimensions.	13
10	Inner race dimensions.	14
11	High speed bearing test rig.	16
12	Assembled bearing test rig and drive turbine.	17
13	Test facility schematic	18
14	Primary instrumentation list.	20
15	Test rig installed in facility.	21
16	Test matrix.	22
17	Oil specific weight and specific heat.	24
18	Measured heat generation data trends.	25
19	Test results summary.	27
20	Race/oil temperature difference (35mm Si <sub>3</sub> N <sub>4</sub> roller bearing)	28

<u>FIGURE NUMBER</u>		<u>PAGE</u>
21	Oil temperature rise (35mm Si <sub>3</sub> N <sub>4</sub> roller bearing).	29
22	Effect of Radial load on Si <sub>3</sub> N <sub>4</sub> roller bearing heat generation.	30
23	Si <sub>3</sub> N <sub>4</sub> roller bearing heat generation (corrected for heat transfer effects).	31
24	Silicon nitride heat generation compared to M50	32
25	Si <sub>3</sub> N <sub>4</sub> roller bearing before testing.	34
26	Si <sub>3</sub> N <sub>4</sub> roller bearing after testing.	35
27	Inner race defect, 12X	36
28	Inner race defect, 160X, SEM.	36
29	Inner raceway dent, 12X.	37
30	Inner raceway axial profiles.	38
31	Outer raceway axial profiles.	40
32	Inner race rib wall profiles.	41
33	Typical roller crown profiles.	42
34	Silicon nitride roller surface outside (A) and within (B) load zone, 500X, SEM.	43
A1	RCF test results on billets of inferior fatigue life (800 ksi contact stress).	46
A2	Chemical analyses (w/o) of NC-132 silicon nitride billets.	46
A3	Etch pit (white central spot) on RCF rod, 500X.	47
A4	Si <sub>3</sub> N <sub>4</sub> microstructures of material performing well (A) and poorly (B), 5000X, SEM.	48
A5	Silicon nitride fracture energies and fatigue lives.	50
A6	Si <sub>3</sub> N <sub>4</sub> fatigue life (Method II versus fracture energy DCB).	52

## FOREWORD

This report covers activities carried out by Norton Company, Worcester, Massachusetts, 01606, under Naval Air Systems Command Contract N00019-75-C-0197, to investigate the utility of silicon nitride in rolling contact bearings. The work was administered under the direction of Mr. Charles F. Bersch, NAVAIR, Washington D.C.

The following Norton personnel were major contributors to the program in the capacity noted.

H. R. Baumgartner - Principal Investigator  
M. L. Torti - Technical Management

Federal Mogul Corporation, Ann Arbor, Michigan, 48104, and Pratt and Whitney Aircraft, West Palm Beach, Florida, 33402, were subcontractors to Norton Company. Both contributed to bearing design. In addition, Federal Mogul and Pratt and Whitney were responsible for bearing fabrication and testing, respectively.

P. E. Cowley - Program Manager, Federal Mogul  
G. S. Calvert - Program Manager, Pratt and Whitney

The authors wish to thank Dr. Stephen Freiman of the Naval Research Laboratory for measuring the critical stress intensity factors of the silicon nitrides.

## ABSTRACT

The objectives of the program were to design, fabricate and evaluate the performance of a roller bearing having hot-pressed silicon nitride rollers and steel races at speeds up to 71,500 rpm (2.5 million DN). The 35mm bore bearing consists of AISI CVM M50 steel races, fourteen fully crowned NC-132 silicon nitride rollers and a silver plated AMS 6414 steel retainer.

Bearing performance was defined in terms of operating temperature, heat generation and vibration at speeds between 30,000 and 71,500 rpm under a predominately 130 pound radial load. Following the calibration testing, the bearing was endurance tested an additional 19 hours at 71,500 rpm.

The bearing test operation was smooth and trouble-free. Heat generation of the silicon nitride roller bearing was comparable to that of a similar M50 steel roller bearing.

Post-test bearing inspection showed the bearing to be in generally good condition with the major exception of a crack in the inner steel raceway that was caused by the interaction of a contamination dent and a carbide inclusion. Some roller wobble had occurred, as indicated by retainer pocket wear.

## SUMMARY

The program investigated the application of silicon nitride bearing components in rolling contact bearings. The goals of the programs were to design, fabricate and define the performance of an aircraft quality, roller bearing containing hot-pressed silicon nitride rollers and conventional steel races in high speed operation.

The design for the bearing is a modification of an existing steel bearing currently used in an engine application. Modifications to the all-steel bearing design were restricted to those items considered essential for a 2.5 million DN speed and the use of silicon nitride roller elements. Aside from the use of silicon nitride, the major alterations involved the internal clearance and the outer race-to-housing fit. Firstly, the unmounted internal clearance was set at 0.0030 - 0.0035 inch to compensate for the lower relative thermal expansion of silicon nitride to steel. Secondly, the roundness of the outer race diameter was made perfectly round. The steel bearing has a slightly eccentric outer diameter so that the bearing experiences a preload when it is installed in its housing. The purpose of this "pinch" is to prevent roller element skidding during certain engine conditions. As the preloading could be accomplished in the test rig, the outer race was made round to simplify manufacture.

The 35mm bore bearing utilized AISI CVM M50 steel for the races. The inner race is double ribbed and the outer race is straight. The retainer is a one piece, separable type made of AMS 2412 steel with a silver plating. The rolling element complement consists of fourteen fully crowned NC-132 silicon nitride rollers.

The silicon nitride material used in the program was qualified by strength testing and rolling contact fatigue (RCF) measurements. The ceramic had a four-point bend strength of 120 ksi. Ten RCF tests were performed at a nominal compressive stress level of 800,000 psi. Only one test, at 10.5 million stress cycles, resulted in element failure; the remaining tests were suspended shortly after 25 million stress cycles.

The fracture energies for a series of previously RCF tested silicon nitrides were obtained by a double cantilever beam technique. Higher fracture energies for the ceramic were found to correlate with longer fatigue lives. The RCF element test machine was also used to investigate the possibility of improving the fatigue life of silicon nitride by annealing it to remove finishing related residual stresses. Preliminary RCF test results did not indicate an enhanced fatigue life and the ceramic rollers for the test bearing were left in the unannealed state.

To manufacture the silicon nitride rollers, length finished cylindrical blanks with radiused end corners were prepared initially by diamond grinding and lapping techniques. The roller blanks were given a full crown, of 18 inch radius, by plunge grinding with a dress-formed silicon carbide wheel on a centerless grinder. Between 0.0003 inch and 0.0006 inch, depending on location along roller axis, of radial silicon nitride stock was removed in this operation. After crowning, the rollers were individually blended at the corner radius-outer diameter and corner radius-end intersections by a diamond lapping operation to minimize stress concentrations. Two roller sets of fourteen size-matched rollers each were selected for bearing assembly. Within each set, the extreme ends of the diameter size range differed by only 0.0004 inch.

The steel races were manufactured from steel rod stock by conventional methods. Eleven inner and eleven outer races were initiated, of which five of each were scraped in-process for various dimensional deviations. The steel retainers were fabricated without incident.

Two bearings were assembled from the best components. The bearings met or exceeded all design specification tolerances. The measured radial internal clearance of the test assembly was 0.0034 inch.

The operating characteristics of the roller bearing were defined with a fully instrumented test rig which was capable of rotational speeds in excess of 72,000 rpm. Thermocouples were used to measure outer race temperature and oil supply and exit temperatures. Other instrumentation measured oil supply flows, vibration levels and shaft speed. Radial load on the roller bearing was applied by a pressurized piston that acts on the outer race. The inlet temperature of the oil (MIL-L-23699B specification) was kept constant at 150°F.

The bearing test matrix and results are summarized in Figure S1. The data points comprise the calibration test used to define operating characteristics. The first fifteen data points were used to determine operating temperature and bearing heat generation as a function of speed and oil flow. Points 16 and 17 provided data at two additional radial loads. Following the calibration test, the bearing was endurance tested an additional 19 hours at 71,500 rpm and 130 pound radial load.

Throughout the test program, vibration levels, operating temperature and speed remained constant over time for a given test condition, which indicated no bearing deterioration. The trends of a) the temperature difference between the outer race and the oil and b) the oil temperature rise as a function of speed and oil flow were as expected.



Point (#)	Speed (1000 RPM)	Radial Load (lb)	Oil Flow (lb/min)	Oil $\Delta T$ ( $^{\circ}F$ )	Out. Race/Oil $\Delta T$ ( $^{\circ}F$ )	Roller Bearing Q (BTU/MIN)
1	30	130	3.9	35	39	75
2	30	130	2.5	36	41	62
3	30	130	1.1	45	51	50
4	45	130	3.9	63	74	131
5	45	130	2.5	71	83	93
6	45	130	1.1	81	93	66
7	65.3	130	5.9	98	116	268
8	65.3	130	4.9	99	119	229
9	65.3	130	3.9	102	121	190
10	65.3	130	2.5	112	132	154
11	71.5	130	5.8	110	133	295
12	71.5	130	4.9	112	134	256
13	71.5	130	3.9	116	138	225
14	71.5	130	2.5	128	149	177
15	71.5	130	2.0	129	150	156
16	71.5	100	3.8	119	140	228
17	71.5	160	3.9	116	137	221

FIGURE S1. Bearing calibration test matrix and summary of results.

Corrected heat generation data,  $Q$ , for the roller bearing are also compiled in Figure S1. The measured heat generation data were corrected for heat transfer effects between the test bearing and a support bearing with the use of heat generation data previously determined for the support bearing. Heat generation trends of the roller bearing were as expected. More importantly, the heat generation of the silicon nitride roller bearing was found to be comparable to that of a similar M50 steel roller bearing at 65,300 rpm. The heat generation of the silicon nitride roller bearing was essentially independent of radial load over the range of 100 to 160 pounds.

After testing, the bearing was examined for its general condition. With one major exception, the bearing condition was good. An axial crack was found in the inner raceway. This crack was caused by the interaction of a contamination dent with a stringer inclusion. Other evidence for contaminate particles were other indentations and scoring on one race guide land. Both raceways were free of any significant wear and the internal clearance of the bearing was unchanged by testing. There was no evidence of lubrication related surface distress on either raceway.

The retainer showed heavy roller contact and the "dog-bone" wear pattern characteristic of roller wobble. The wobble polished the top third of the inner race roller guide ribs, but did not cause any abnormal wear on the ribs.

The silicon nitride rollers were in excellent condition and showed no visible wear or surface degradation.

## I INTRODUCTION

Ceramic materials offer many properties which suggest their use in bearings. Among these are: light weight, high mechanical strength in compression, resistance to corrosion, low coefficient of friction, dimensional stability, and high hardness over a wide temperature range. In addition they are generally further characterized by high resistance to wear, low coefficient of thermal expansion, very high melting point, and the ability to hold close tolerances and fine finishes. Because of the desirability of many of these properties, extensive studies have been conducted with both solid ceramic and ceramic coatings for sliding and plain bearing in industry.

Until relatively recent times, ceramics have performed poorly under rolling contact bearing conditions. Contact fatigue studies with crystallized glass<sup>1</sup>, various forms of alumina<sup>2,3</sup> and forms of silicon carbide<sup>2,3</sup> resulted in lives of less than 10 percent of bearing steels. Hot-pressed silicon nitride, however, is a ceramic which has emerged with outstanding rolling contact fatigue life.

The density of hot pressed silicon nitride is approximately two-fifths that of steel. At high turbine engine speeds, the loading on the outer bearing race due to the centrifugal forces exerted by the rolling elements becomes important. The lower density of silicon nitride rolling elements would reduce this centrifugal loading.

The attributes of good fatigue life and low density have led to many investigations of hot pressed silicon nitride as a bearing material. Element ball tests have shown silicon nitride to have a fatigue life equivalent to that of a typical bearing steel.<sup>4</sup> Roller element tests<sup>3,5</sup> have shown hot pressed silicon nitride to have fatigue lives significantly superior to bearing steel. The lubrication and frictional characteristics of silicon nitride have been studied.<sup>6</sup> The importance of surface preparation<sup>3,7</sup> and material properties<sup>3,8</sup>, such as high density and microstructural uniformity, on long fatigue life has been stressed.

The feasibility of using silicon nitride in full scale bearings has been demonstrated<sup>8</sup> with an all-silicon nitride roller bearing and a roller bearing containing ceramic rolling elements and steel races. Additional characterization<sup>9</sup> has been made of a group of bearings, with steel races and silicon nitride rollers, operating under heavy load and moderate speed.

Recently, the performance of a 35mm bearing, with hot pressed silicon nitride balls and M50 steel races, operating at speeds to 71,500 rpm (2.5 million DN) has been reported.<sup>10</sup> The heat generation of the bearing was 10 to 20 percent less than that of a comparable bearing with steel balls and required a lower load to prevent ball skidding.

The objectives of the current program were to a) demonstrate the feasibility of designing, fabricating and operating a bearing with silicon nitride rollers and steel races at speeds up to 2.5 million DN and conditions typical of advanced small gas turbine engines and b) to characterize bearing performance in terms of operating temperature, heat generation and vibration levels.

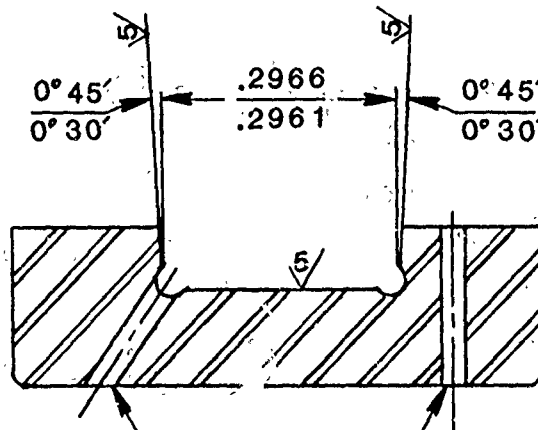
## II BEARING DESIGN

The bearing used in the program was jointly designed by Pratt and Whitney Aircraft and Federal Mogul. The bearing was intended as a possible replacement for an existing steel bearing (Bower part number KU-73518-CJ) currently used in a Navy engine. This latter bearing has a life of 1600 hours as compared to a desired life of 5000-10000 hours. Modifications to the all-steel bearing design were limited to those items considered essential for a 2.5 million DN speed and the use of silicon nitride rolling elements. The modified bearing is identified as KX208 and is shown in Figure 1. The bearing has a 35mm bore, a double ribbed inner race and a straight outer race. The steel race material is AISI CVM M50 steel. The inner race employs radial lubrication holes for centrifugally injecting lubricant from under the race to the raceway-rib intersection and the cage guidance lands. Fourteen fully crowned rollers of hot-pressed NC-132 silicon nitride are used. The cage is a one piece, separable type and is of silver plated steel.

Aside from the rollers, the major design alterations involved the unmounted internal clearance and the outer race-to-housing fit; the inner race-to-shaft fit remained as 0.0016" tight/0.0024" tight. The unmounted internal clearance was revised to 0.003-0.0035" to compensate for the lower thermal expansion of silicon nitride relative to steel ( $1.7 \times 10^{-6}$  versus  $6.5 \times 10^{-6}$  in/in°F). The design operating internal clearance is 0.001" to 0.0027", depending upon bearing and fit tolerances. The second major alteration involved the shape of the outer race. The outer race of the all-steel bearing normally has a 0.006" out-of-round outer diameter so that the bearing experiences a preload "pinch" when it is installed in its housing. The purpose of the preload is to prevent roller skidding during low loading conditions, such as engine start-up or zero "g" force conditions during certain aircraft maneuvers. The outer race for the current bearing was finished round to facilitate manufacture as the test rig could be externally loaded to supply the anti-skid preload.

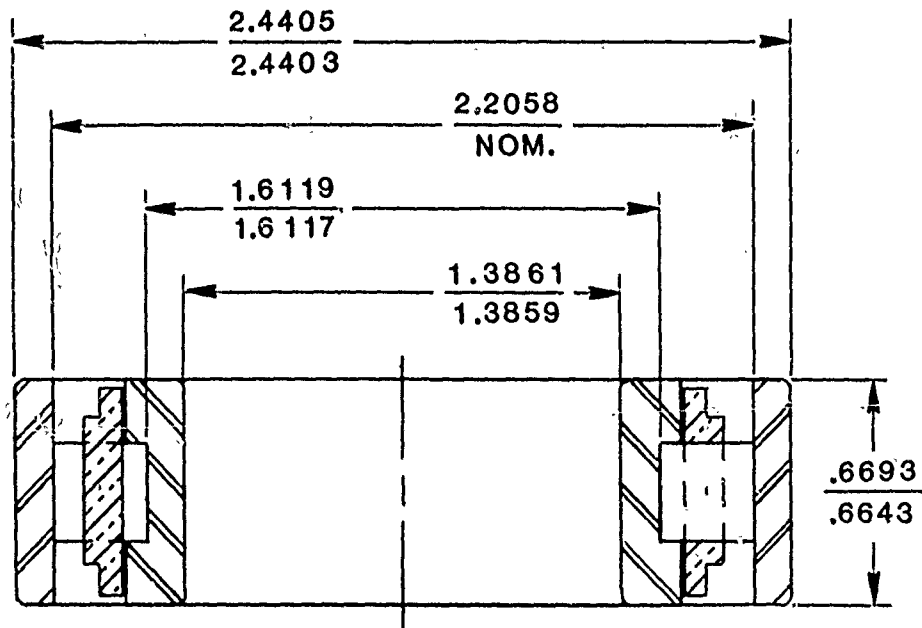
The detail of the silicon nitride roller geometry is shown in Figure 2. A fully crowned roller was chosen to avoid premature race failure due to a stress concentration possibly developing at the intersection of a partial roller crown and the flat. This occurrence is potentially more likely with silicon nitride elements because of its relatively high modulus (thus causing


# ENLARGED VIEW OF INNER RACE SECTION



.037/.030 DIA. 12 HOLES  
EQUALLY SPACED,  
6 HOLES ON EACH SIDE  
OF TRACK FROM BORE  
TO RECESS

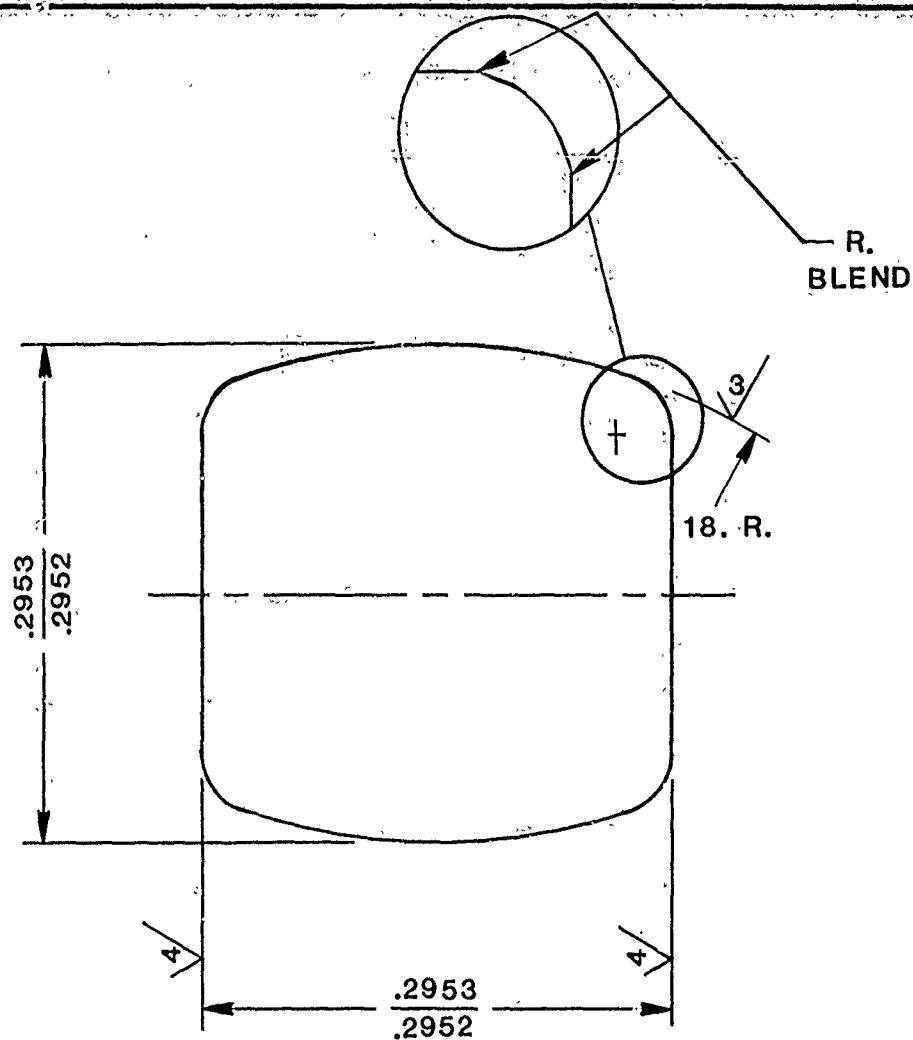
.037/.030 DIA. 4 HOLES,  
2 ON EACH SHOULDER  
LOCATED 180° APART



SUPERSEDES			LOAD RATING BY AFBMA METHOD 500 HRS L-10 LIFE AT 500 RPM		R.B.E.C. 5 CLASS
SUPERSEDED BY			RADIAL 2415 LBS.		
	DWN	CKD	<b>FEDERAL-MOQUIL</b> BEARING GROUP 		BEARING NO.
DATE	7-7-76				KX-208
BY	R. MYNAR				

POST 2308-1a

FIGURE 1 - Design of test bearing KX-208.



14 ROLLERS REQUIRED PER BEARING  
 MATERIAL: SILICON NITRIDE NC-132  
 DIAMETER VARIATION NOT TO EXCEED .000050  
 LENGTH VARIATION NOT TO EXCEED .0001  
 O.D. ROUND WITHIN .000025

SUPERSEDES			SCALE NONE	
SUPERSEDED BY				
	DWN	CKD	ROLLER NO.	
DATE	7-7-76		KX-208-3	
BY	2.61TMC			

**FEDERAL-MOGUL**  
 BEARING GROUP



POST 2308-1a

FIGURE 2 - Detail of silicon nitride roller geometry.

relatively more deformation in the softer race material) and the manufacturing difficulty of achieving a well blended intersection.

Use of the bearing at 3 million DN was also evaluated. Roller form and internal clearance are satisfactory. However, the inner race-to-shaft fit would have to be selected to the high side of the tolerance to maintain a tight fit.

Inner race hoop stresses due to the interference fit and the centrifugal load is 24 ksi at 71,500 rpm (2.5 million DN) and 27 ksi at 85,700 rpm (3 million DN). These stresses are somewhat above normal for through hardened bearing steel (20 ksi), but are below that of case-hardened steel (30 ksi).

### III SILICON NITRIDE MATERIAL CHARACTERIZATION

The suitability of the NC-132 silicon nitride material for bearing components was evaluated by strength testing, density, and rolling contact fatigue life. The billet material had a bulk density 3.23 g/cc and a mean strength, as measured in four-point bending, of 119.8 ksi. Additional strength testing details are presented in Figure 3.

Material: NC-132 silicon nitride; Billet #438756

Specimen Size: 0.125" x 0.250" x 2"

Method of Test: Four-point bending

Test Fixture Spans: 0.75" over 1.50"

Fracture #	Strength (ksi)	Fracture #	Strength (ksi)
1	98.9	6	118.1
2	143.9	7	120.0
3	113.7	8	135.1
4	126.3	9	140.1
5	128.0	10	74.2

Mean Strength = 119.8 ksi

Standard Strength Deviation = 20.8 ksi

FIGURE 3 - Strength qualification data for silicon nitride roller stock.

The rolling Contact Fatigue (RCF) test machine, shown in Figure 4, was used to evaluate the rolling contact fatigue behavior of the silicon nitride used in this program. In previous programs,<sup>3,7,8,9</sup> the RCF test was found to be useful in evaluating the fatigue behavior of various silicon nitrides and the effect of silicon nitride finishing techniques. During the RCF test, two steel discs, each with a 0.250" crown radius, are pressed against a rotating test specimen. The test specimen is a three inch long cylinder of 0.375" diameter and is rotated at 10,000 rpm. The nominal (unlubricated) contact stress may be calculated from the geometrical contact configuration and the applied load.<sup>8</sup> For a steel test specimen, a 325 pound load results in a nominal maximum compressive contact stress of 700 ksi. The same load produces a maximum stress of 800 ksi when a silicon nitride specimen is used, due to the higher modulus of elasticity of the ceramic. A Type II Turbo Oil of Military Specification MIL-L-23699B is used as a drip lubricant. The test machine is qualified as a system by the use of a controlled lot of CVM M50 steel specimens, termed "Q"-bars, and whose fatigue lives normally range between 1.5 and 4 million stress cycles for the standard 325 pound load. The loading discs are refinished when they spall or flatten, after which the system is requalified.

The RCF qualification tests on silicon nitride were conducted to ensure against the possible use of sub-standard material in terms of rolling contact fatigue performance. Indeed, as is discussed at length in Appendix I, the initial silicon nitride material intended for program use was disqualified on the basis of its poor RCF performance. The emphasis of RCF testing is on the detection of "early" failures. While the duration of an "early" failure is somewhat arbitrary, certainly lives less than that of the "Q" bars are suspect. Fatigue lives in excess of 30 million stress cycles at a 800 ksi stress level are common for NC-132 silicon nitride, although occasional (10 percent or less of the tests) "early" failures have been experienced.

Two silicon nitride RCF specimens were prepared from the NC-132 billet #438756 by diamond grinding. Bar stock was rough ground to an approximately 0.010" oversize diameter with a 150 grit, resinoid bonded diamond wheel. Further OD grinding with a 320 grit resinoid bonded diamond wheel (specification number SD320R100B69) was used to remove 0.010" of stock. All grinding was done with a water based coolant, wheel speed of 5500 sfpm, work speed of 600 rpm and a traverse rate of 0.001" per work revolution. An infeed of 0.00025"/pass was used for the first 0.008" of stock removal with the 320 grit wheel and was reduced to 0.0001"/pass for the last 0.002" of stock removal. The rods were finished with a 400 grit diamond OD hone, using honing oil, to reduce the final surface roughness and improve rod concentricity. Finish characteristics of the RCF specimens are presented in Figure 5.



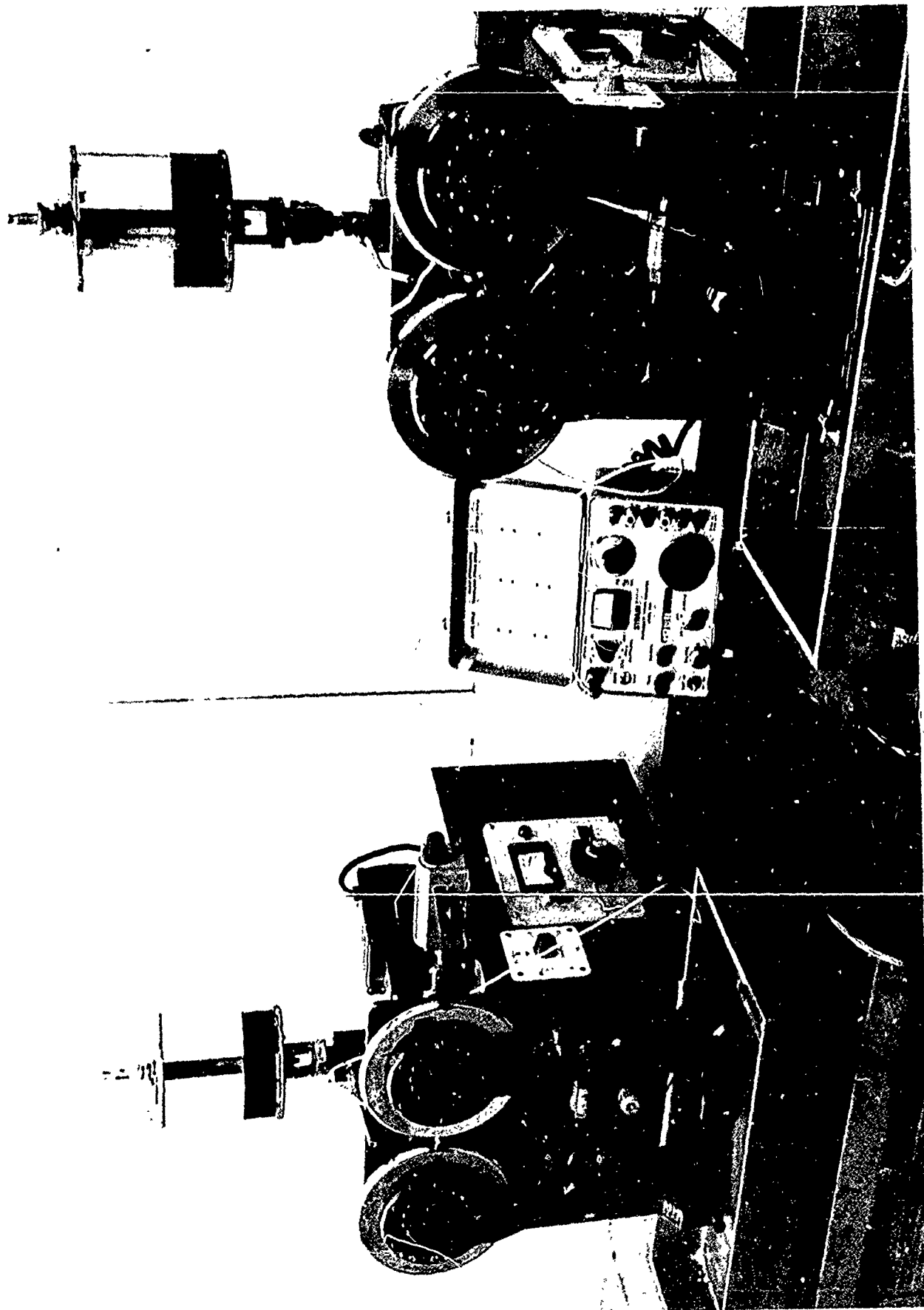


FIGURE 4 - Rolling Contact Fatigue (RCF) test machine

<u>Specimen Rod</u>	<u>Surface Finish (Micro Inches, AA)</u>		<u>Departure from Roundness (Micro Inches)</u>
	<u>Axial</u>	<u>Circumferential</u>	
#1	1.5 - 2.5	1.5 - 3.0	20
#2	2.5 - 5.5	2.0 - 4.0	60

FIGURE 5 - Finish characteristics of silicon nitride RCF specimens.

A total of ten fatigue tests were performed on the two specimens at a 800 ksi contact stress level. If the specimen did not fail before twenty-five million stress cycles, the test was suspended. The RCF test results are shown in Figure 6. The material exhibited adequate fatigue resistance as is demonstrated by only one fatigue failure at 10.5 million stress cycles.

<u>Rod #</u>	<u>Test #</u>	<u>Life (<math>10^6</math> cycles)</u>	
1	1	10.5	
	2	27.8	Suspended Test
	3	26.0	" "
	4	26.1	" "
	5	25.3	" "
2	1	27.2	" "
	2	26.3	" "
	3	25.1	" "
	4	27.9	" "
	5	25.4	" "

FIGURE 6 - Fatigue life results for silicon nitride Billet #438756 at 800 ksi stress

In an attempt to explain the inability of the initial silicon material to qualify under the RCF test, substantial silicon nitride characterization was performed. As mentioned above, this work is reported in Appendix I. Because of its importance to the theory of rolling contact fatigue of silicon nitride, it is mentioned here that a positive correlation was found between the rolling contact fatigue resistance and the effective fracture energy of silicon nitride.

#### IV BEARING FABRICATION

##### A. Roller Manufacture

The material of the bearing rollers is hot-pressed NC-132 silicon nitride. The rollers were fabricated in two phases.

In the first fabrication phase, one hundred and twenty straight cylindrical roller "blanks" were produced by diamond grinding techniques. Square bars 0.4" x 0.4" x 6" were sliced from the original billet and ground to 0.355" rounds using a 150 diamond grit, resinoid bonded wheel. The rods were then taken to 0.2970" + 0.0002" on a centerless grinder employing a 220 diamond grit, resinoid bonded wheel. The rods were ring lapped with six micron diamond paste to make them round to within twenty-five micro-inches. The rods were sliced to two inch lengths, machine roll-lapped to 0.2958" ± 0.0001" diameter with six micron diamond paste, and then sliced into 0.299" - 0.0002" lengths. The cylindrical ends were surface ground flat and parallel with a 320 diamond grit, resinoid bonded wheel, which was also used to generate the corner radii. A water-based coolant was used in all grinding operations.

Following manufacture, the roller blanks were inspected for their geometry. Figure 7 lists the specified and actual dimensions of the roller blanks; all specifications were met.

In the second phase, the roller crown profile was plunge ground onto the blanks using a centerless grinder with a silicon carbide wheel (specification GC-150-L-10V5). The roller blanks are oversize 0.0003" per side. The specified crown radius (18") requires twice as much stock to be removed toward the ends of the rollers (0.0006") as is removed in the center (0.0003"). To attain the specified 18" radius, it was found to be necessary to dress the grinding wheel to a 14" radius and take two cuts. The first cut removed more stock from near the ends of the roller to intentionally leave a more uniform layer of stock to be removed by the second cut. The second cut finished the profile and size. The grinding wheel was re-dressed after approximately every five roller cuts. The resultant crown profiles were exceptionally uniform.

<u>Characteristic</u>	<u>Specification</u>	<u>Actual</u>
Diameter	0.2959/0.2957	0.29585/0.29580
Length	0.2953/0.2952	0.2953/0.29525
Roundness	0.000025 T.I.R.	0.000025 max.
End Squareness	0.0001 T.I.R.	0.00008/0.00002
End Parallelism	0.0001 T.I.R.	0.00008/0.00002
Corner Radius	0.038/0.033	0.034/0.030
Corner Radius Concentricity	0.0005	0.0005 max.
Diameter Surface Finish	3 AA max.	2-3 AA
End Surface Finish	4 AA max.	2-3.5 AA

Dimensions are in inches except for finishes which are in micro-inches.

FIGURE 7 - Roller blank dimensions

The principal problems experienced involved maintaining roundness and diametral size. The roundness problem is attributed to the roller's small size and the material's light weight which increased the tendency to chatter. Very small coolant flows tended to "wash" the rollers out of position. The difficulty of maintaining the required size is attributed to the combination of the small lot size, the frequent re-dressing required, and the close tolerances involved.

Two roller sets of 14 rollers each were selected for the test bearing and a back-up bearing. The two sets were the same general quality, the only difference being their group size. Their specified and actual dimensions are listed in Figure 8.

After the crowning operation, the rollers in Sets 1 and 2 were individually blended at the intersection of the corner radius and the body diameter and at the intersection of the corner radius and the end in order to minimize stress concentrations. Blending was achieved by lapping with 10 micron, followed by six micron, diamond paste.

<u>Characteristics</u>	<u>Specification</u>	<u>Set 1</u>	<u>Set 2</u>
Size	0.2953/ 0.2952	0.29529/ 0.29525	0.20525/ 0.29521
Crown Height	0.00031/ 0.00021	OK	OK
Crown Centrality	0.020 T.I.R.	0.010 max.	0.010 max.
Roundness	0.000025	0.000025/ 0.000010	0.000025/ 0.000010
Waviness (3-Point Chk.)	0.000025	0.000025/ 0.00000	0.000025/ 0.00000
Chatter (2-Point Chk.)	0.00002	0.000025/ 0.00001	0.000025/ 0.00001
Surface Finish	3 AA max.	2-3 AA	2-3 AA
Max. Diameter Variation	0.000050	0.000040	0.000040
Max. Length Variation	0.0001	0.00006	0.00006

Dimensions are in inches except for finish  
which are in micro-inches

FIGURE 8 - Crowned roller dimensions

The finished rollers were inspected with a fluorescent dye penetrant and showed no defect indications. In an additional inspection, a random sample of eight rollers, four from each set, were examined by scanning electron microscopy for microcracks near the roller corners. The corners were inspected as they are believed to have been the origin of roller spalls in previously<sup>9</sup> tested bearings. No evidence of cracking was found.

It has been demonstrated<sup>11</sup> that estimates of the critical stress intensity factor,  $K_{IC}$ , for silicon nitride may be obtained from a method involving bend fractures which initiate from characterized Knoop indenter flaws. For unannealed specimens, the apparent  $K_I$  values are substantially less than values obtained upon annealed specimens. The latter results agree well with  $K_{IC}$  data obtained by other methods. An explanation for the effect of annealing on apparent  $K_{IC}$  was based upon the relieving of residual tensile stresses at the tip of the induced crack.

Since sub-surface microcracks are introduced as machining damage and it is possible that the finished surfaces may possess residual stresses, the effect of annealing on the rolling contact fatigue of silicon nitride was investigated. Roller Set #2, together with a previously tested<sup>12</sup> RCF rod, were treated at 1250°C for four hours under a nitrogen atmosphere. The thermally processed RCF rod belonged to a control group of similarly processed and tested specimens. This group had eleven fatigue failures at an 800 ksi stress level with the lives ranging from 1.35 to 47.4 million stress cycles and an L<sub>10</sub> life of 1.5 million cycles. Four additional RCF tests were performed on the annealed rod with fatigue failures after 0.15, 0.90, 3.4 and 5.7 million stress cycles. These new test results are poor and apparently inferior to the prior unannealed lives. For this reason, the annealed set of rollers were not used for the test bearing. It is felt that the effect of a thermal stress relief treatment on stress fatigue requires a more extensive evaluation.

#### B. Race Manufacture

The inner and outer races were fabricated from AIST CVM M50 (PWA Specification 725B) steel bar stock by standard methods. Eleven inner and eleven outer races were initiated, of which five of each were scraped in-process for various dimensional deviations. The critical dimensions of the remaining six candidate outer races are listed in Figure 9 and the six candidate inner races in Figure 10. The finished races were etch inspected for grinding burns and magnetic particle inspected for cracks and inclusions. Their hardnesses were Rockwell 'C' 61 - 62.

#### C. Retainers

The cages were fabricated without incident. The retainer material was AMS 6414 steel, hardened to Rockwell C 28-34, and was covered with a 0.001" - 0.002" thick silver plating.

#### D. Bearing Assembly

The components selected for the test bearing assembly consisted of inner race letter A, outer race number 6 and roller set number 1. The measured radial internal clearance of the assembly was 0.0034", within the 0.0030" to 0.0035" specification. A second bearing, containing the annealed rollers, was assembled, but not tested.

Characteristic	Spec.	Race No.				
		1	3	4	5	6
Outside Diameter	2.4405 2.4403	2.4404	2.4404	2.4404	2.4404	2.44038
Outside Roundness		0.00009	0.00004	0.00008	0.00008	0.00004
Thickness Variation	0.0002 max.	0.00005	0.00006	0.00004	0.00003	0.00005
Raceway Diameter	2.2058	2.20575	2.20563	2.2056	2.20574	2.20555
Raceway Roundness	0.00025	0.00008	0.00005	0.00007	0.00004	0.00003
Raceway Taper	0.00005	0.00005	0.00002	0.00001	0.00004	0.00002
Raceway Surface Finish	5 AA	5 AA	3 AA	3 AA	3 AA	5 AA

Dimensions are in inches except for Finish which are in micro-inches

FIGURE 9 - Outer race dimensions.

Characteristic	Spec.	Race No.					
		A	C	E	F	G	K
Bore Diameter	1.3861 1.3859	1.38595	1.38615	1.38589	1.38600	1.38589	1.38615
Bore Roundness		0.00001	0.00001	0.00001	0.00002	0.00001	0.00001
Bore Taper		0.00001	0.00003	0.0001 High Center	0.0002 Shoulder	0.00015 Step	0.0004
Raceway Diameter	1.6119 1.6117	1.6118	1.61193	1.6119	1.6117	1.61183	Not Finished
Raceway Roundness	0.00015 max.	0.00002	0.000025	0.00002	0.0001	0.000025	
Raceway Taper	0.00005 max.	0.00001	0.00004	0.00003	0.00003	0.00002	
Raceway Width	0.2066 0.2961	0.2966	Rib not finished	0.2966	Rib not finished	0.2966	
Bore/Raceway Concentricity	0.0001 max.	0.00003	0.00001	0.00003	0.00001	0.00005	
Raceway Surface Finish	5 AA max.	5 AA	5 AA	4 AA	5 AA	4 AA	

Dimensions are in inches except for Finish which are in micro-inches

FIGURE 10 - Inner race dimensions



## V BEARING TESTING

### A. Test Rig

A cross section of the bearing test rig is shown in Figure 11. The rig consists of two 35mm ball bearings with a 35mm roller bearing in the center. In this test, two M50 ball bearings were used, and the experimental silicon nitride roller bearing was installed in the center position.

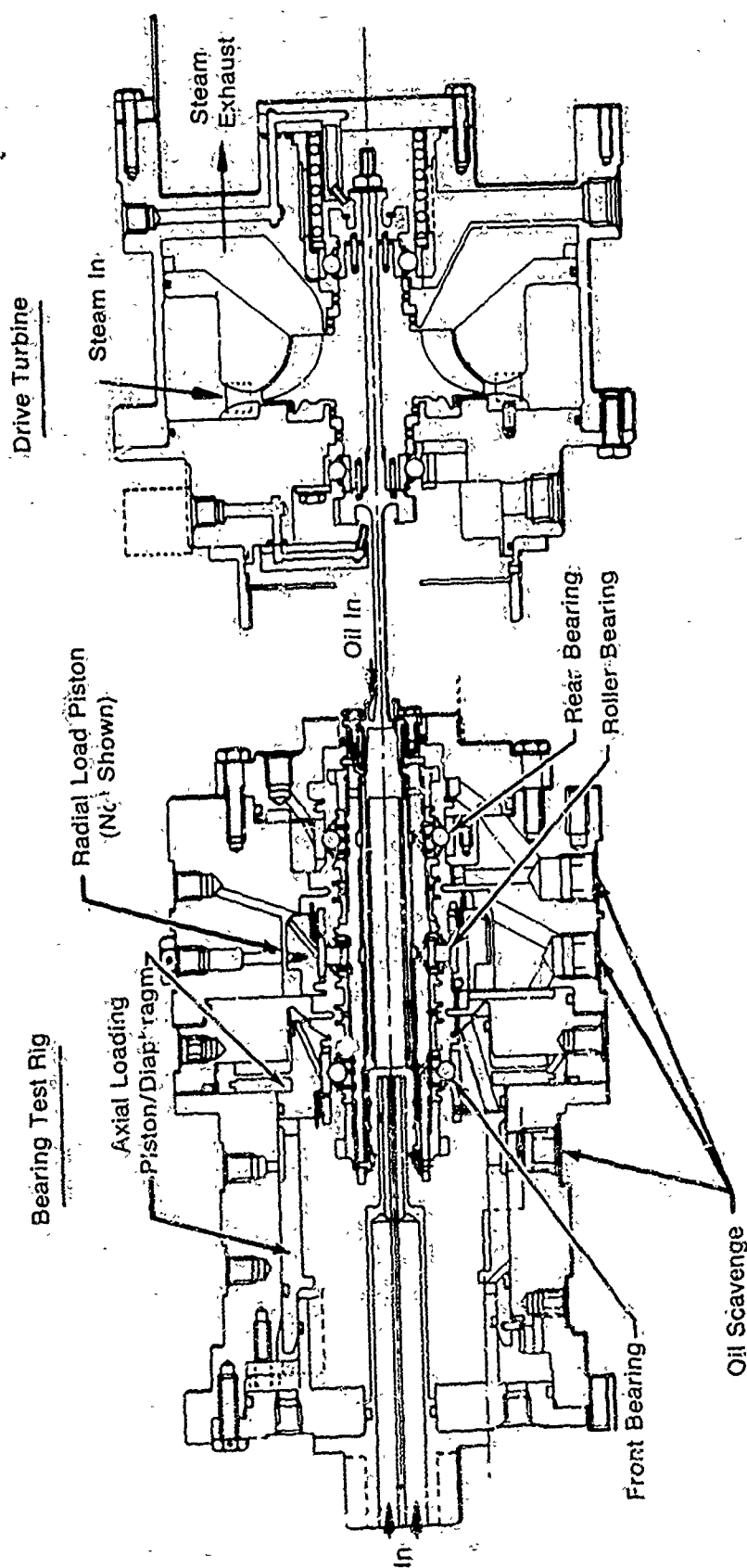
The rig design provides for precise control of axial and radial bearing loads. Ball bearing pre-load is achieved and measured through a strain-gaged diaphragm that has relatively low axial stiffness. Additional axial load in either direction can be applied to the ball bearings by pressurizing either the axial loading piston or the diaphragm. Radial load on the roller bearing was applied by a pressurized piston that acts on the outer race. Since the roller bearing is centered, each of the ball bearings experienced one half the radial load.

Oil was supplied to all three bearings from the inside of the shaft. This oil was supplied separately to each bearing through fixed orifice jets. Oil for the rear ball bearing was supplied from the turbine end, and oil for the front bearing and the roller bearing was supplied from the opposite end. Because the oil for the roller bearing also passes under the front ball bearing, a heat generation correction must be applied to the measured values for these two bearings. (This is discussed under Section V.E.) Once inside the shaft, the oil was separated by slinger type seals, and was pumped through channels and annuli to provide an under-race oil supply to each bearing. Oil discharge flows were scavenged separately for each bearing.

The test rig was driven by a radial inflow stream turbine through a small diameter "quill" shaft. The shaft is capable of absorbing small misalignments without adding load to the test bearings. The drive turbine assembly is self-contained, having its own bearings (of smaller diameter than the test rig bearings) and lubrication system. Figure 12 shows a photograph of the assembled bearing rig and drive turbine. The bearing rig was hard mounted to a baseplate and the drive turbine was supported by three pins, which extended from the bearing rig. Three bushings on the drive turbine allowed the turbine assembly to slide on the pins, preventing the transfer of axial load from the drive turbine to the bearing test rig.

### B. Test Facility

A schematic of the test facility is shown in Figure 13. Oil was pumped from a 25-gal reservoir through a 10 $\mu$  filter to a distribution plenum. Lubricating oil for all bearings was tapped from the plenum and supplied to the components through individual



FD-53302A  
790906

FIGURE 11 - High speed bearing test rig.

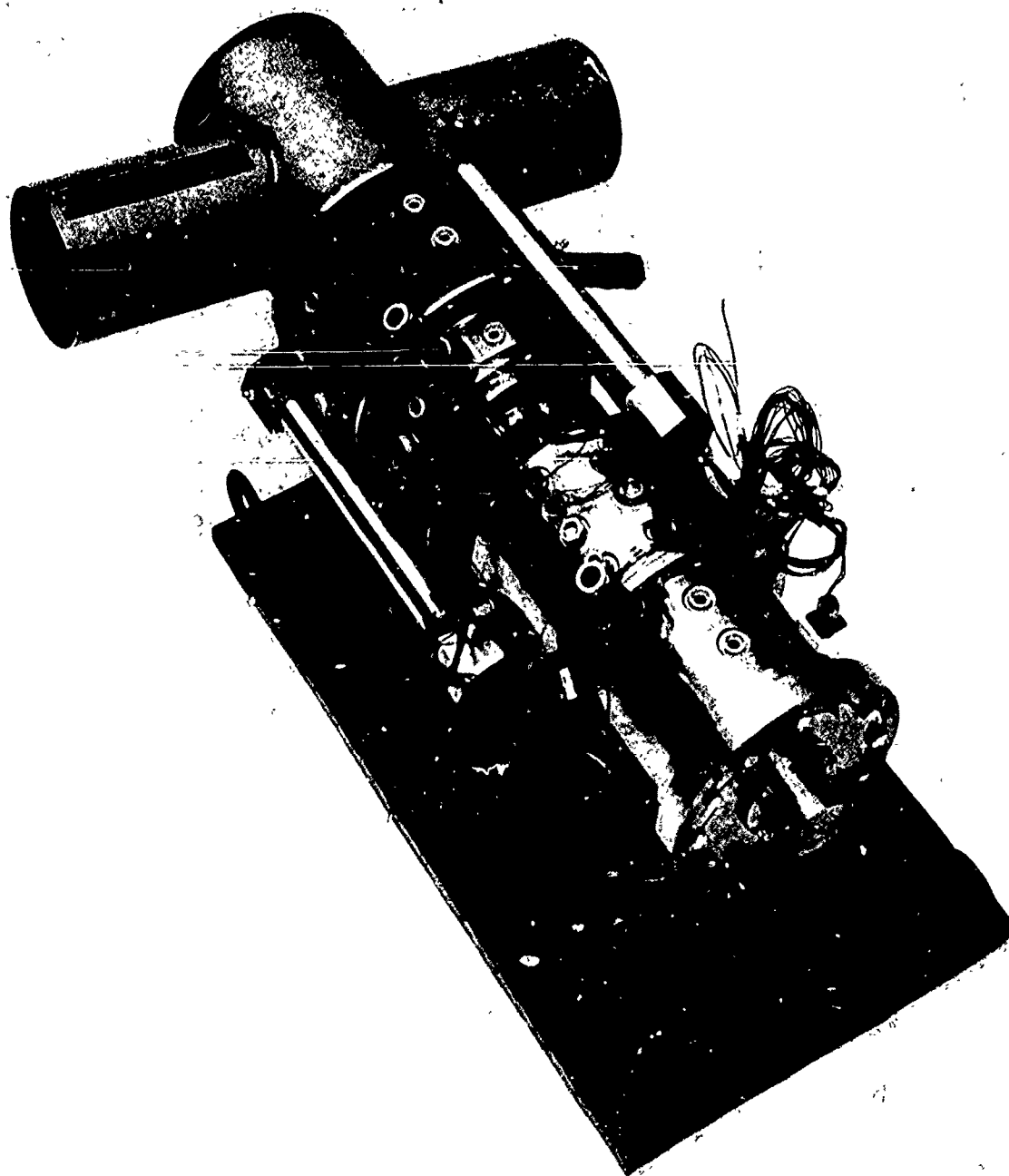
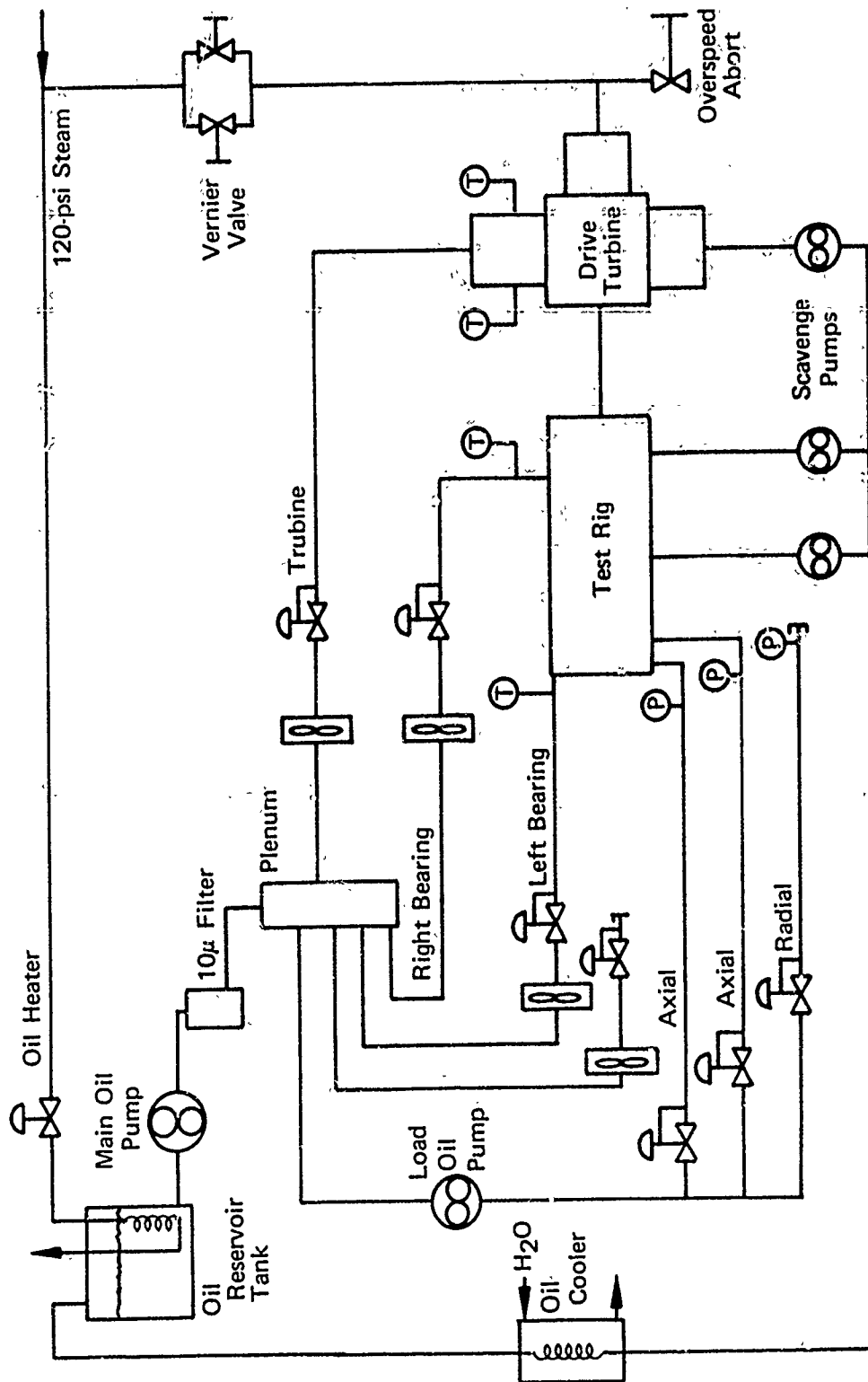


FIGURE 12 - Assembled bearing test rig and drive turbine



F089626

FIGURE 13 - Test facility schematic

flowmeters and control valves. Oil for pressurization of the bearing load pistons was also pumped from the plenum and supplied to the pistons through individual control valves. Bearing oil was scavenged with individual pumps, which discharged into a common line and returned the oil to the reservoir through a water-oil cooler. A steam coil was immersed in the oil reservoir for heating the oil.

Steam was supplied to the drive turbine from an area system through a large control valve and a parallel vernier valve for precise control of speed. The steam supply had provisions for venting itself in the event of a turbine overspeed.

### C. Instrumentation

Primary rig instrumentation is listed in Figure 14. Outer race temperature of the bearings was measured with thermocouples installed in each housing such that they contacted the outer races. Thermocouples were immersed in the oil supply lines and rig sump to measure bearing supply and exit oil temperature. Shaft speed was measured with a magnetic transducer that sensed the passing frequency of a 12-tooth cog on the shaft. Oil flows were measured with turbine-type flowmeters in the supply lines, and rig vibration was measured with accelerometers on the rig housing. All instrumentation is calibrated to standards traceable to the National Bureau of Standards.

### D. Test Procedure

The test rig was installed in the facility as shown in Figure 15 and the oil system was serviced with approximately 25 gallons of oil qualified under the MIL-L-23699B specification. Subsequently, the 50 hour test program described in Figure 16 was completed. The first 15 points were used to obtain operating temperature and heat generation data as functions of speed and oil flow; points 16 and 17 provided data at two different radial loads; and point 18 was the endurance portion of the test. Oil supply temperature was held constant at 150°F for all the tests.

The operating procedure for each day's startup was as follows: circulate and heat the oil to 150°F; apply axial and radial loads to the bearings; set oil flows to each bearing; start rotation and increase rotation, oil flow, and axial load over a period of approximately 20 minutes to the desired test conditions. Subsequent tests were obtained by first changing oil flow, then load, and finally speed, as required. Data were manually recorded every 15 minutes during the tests except during the endurance portion, when data was recorded at 30 minute intervals.

Oil samples were taken from the silicon nitride bearing scavenge line at the end of each day of testing. Spectrographic oil analysis of the samples for iron, nickel, chrome, titanium, aluminum, and copper revealed no measurable increase in these elements.

		SENSOR	
PARAMETER	TYPE		QUANTITY
SPEEDS			
Rig Shaft	Magnetic Transducer		1
Turbine Shaft	" "		1
TEMPERATURES			
Front Bearing Outer Race	C/A Thermocouple		5
Middle Bearing Outer Race	" "		5
Rear Bearing Outer Race	" "		2
Oil Reservoir	" "		1
Front Bearing Oil Supply	" "		1
Middle Bearing Oil Supply	" "		1
Rear Bearing Oil Supply	" "		1
Front Bearing Oil Sump	" "		1
Middle Bearing Oil Sump	" "		1
Rear Bearing Oil Sump	" "		1
PRESSURES			
Axial Load	Gage		1
Radial Load	"		1
Front Bearing Oil Supply	"		1
Middle Bearing Oil Supply	"		1
Rear Bearing Oil Supply	"		1
FLOWS			
Front Bearing Oil Supply	Turbine Flowmeter		1
Middle Bearing Oil Supply	" "		1
Rear Bearing Oil Supply	" "		1
DIAPHRAGM LOAD	Strain Gages		2
VIBRATIONS			
Horizontal	Accelerometer		1
Vertical	"		1

FIGURE 14 - Primary instrumentation list

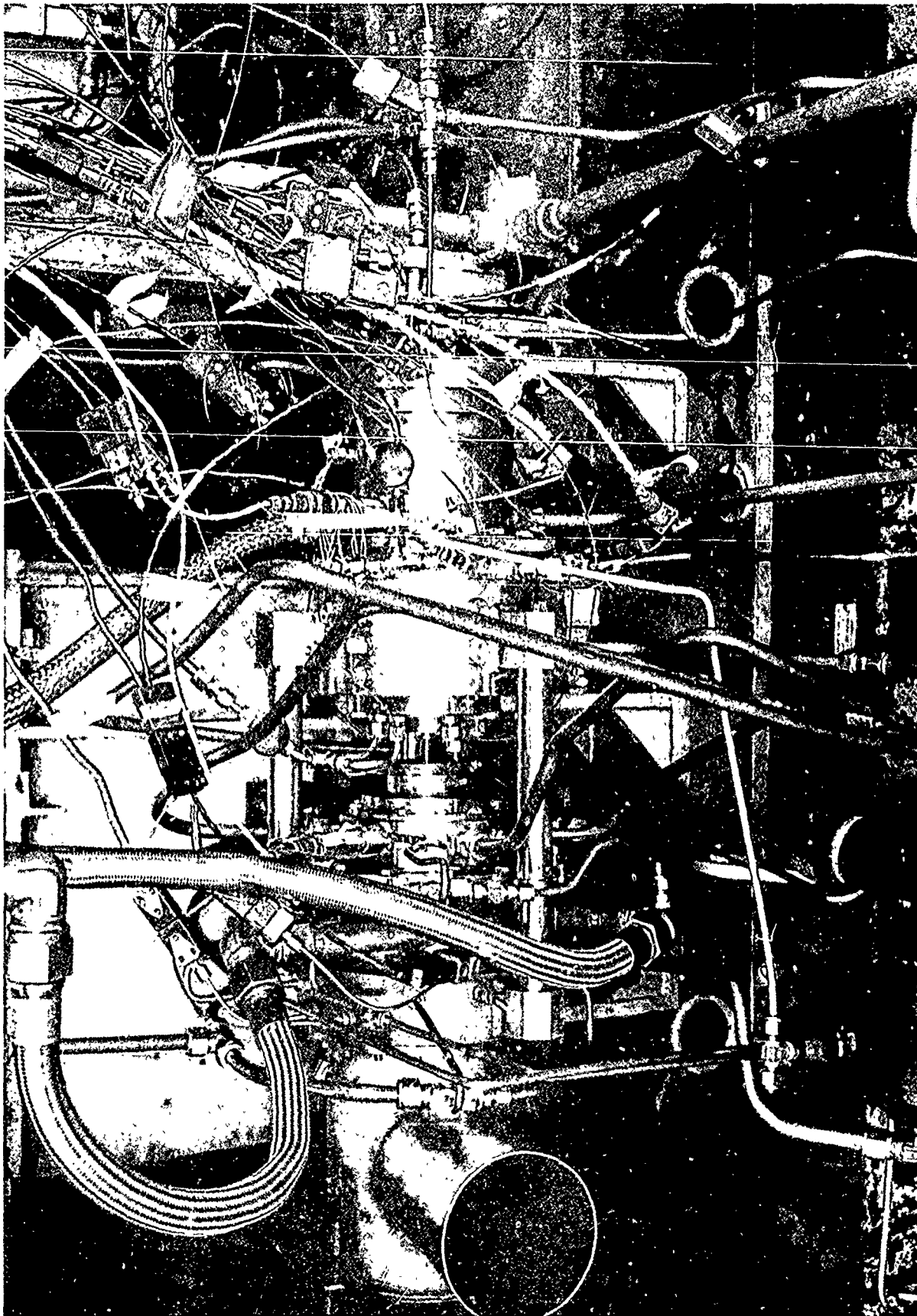


FIGURE 15 - Test rig installed in facility

<u>POINT</u>	<u>SPEED</u> 1000 RPM	<u>RADIAL</u> <u>LOAD</u> lb	<u>OIL FLOW</u> lb/min	<u>DURATION</u> hr	<u>TOTAL @</u> <u>SPEED</u> hr
1	30	130	3.9	2	
2	30	130	2.5	2	
3	30	130	1.1	2	
				<hr/>	6
4	45	130	3.9	2	
5	45	130	2.5	2	
6	45	130	1.1	2	
				<hr/>	6
7	65.3	130	5.9	2	
8	65.3	130	4.9	2	
9	65.3	130	3.9	2	
10	65.3	130	2.5	2	
				<hr/>	8
11	71.5	130	5.8	2	
12	71.5	130	4.9	2	
13	71.5	130	3.9	2	
14	71.5	130	2.5	2	
15	71.5	130	2.0	1	
				<hr/>	9
16	71.5	100	3.8	1	
17	71.5	160	3.9	1	
				<hr/>	2
18*	71.5	130	2.5	19	
				<hr/>	19

TOTAL TEST TIME\*\* - - 50

\* ENDURANCE TEST POINT

\*\* STARTUP AND SHUTDOWN TRANSIENTS CONSUMED ADDITIONAL 3 HRS

FIGURE 16 - Test matrix



### E. Data Reduction Procedure

Volumetric flow data from the turbine flowmeters were converted to weight flow using the refiner's oil specific weight data, and heat generation values were calculated using specific heat data from the same source along with the measured flows and oil temperature rise. The specific weight and specific heat curves used are shown in Figure 17. Bearing loads were calculated from the diaphragm strain gages and piston pressures, as discussed previously. Bearing outer race temperatures were obtained by averaging the thermocouple readings. For a given point, the data were averaged over the entire duration of the test point. Thus, the data for a 2-hour point represents an average of the eight data readings that were taken at 15 minute intervals.

A correction to the measured heat generation ( $Q$ ) of the front bearing and the roller bearing is required to reconcile the test data to known characteristics. For instance, Figure 18 shows typical heat generation data trends for the front and roller bearings. The roller bearing  $Q$  increases linearly as a function of its oil flow, as expected. However, the apparent heat generation of the front bearing decreases with an increase in roller bearing oil flow. This would not occur for a completely adiabatic system, since the parameters that affect  $Q$  (speed, load, oil flow and viscosity) are constant for the front bearing. The heat generation data was corrected by using the known heat generation of the front bearing as measured in a previous program.<sup>10</sup> This is shown as a straight dotted line in Figure 18. (In the previous program, two ball bearings were tested without a roller bearing. Hence, no heat generation corrections were required.) The roller bearing  $Q$  correction factor was determined from the absolute difference between the currently measured  $Q$  and the previously measured  $Q$  for the front bearing. A corrected  $Q$  value for the roller bearing was obtained by adding the correction factor to the measured roller bearing's  $Q$  when the measured  $Q$  of the front bearing exceeded the known value and subtraction when the measured  $Q$  of the front bearing was smaller than the known value.

The heat transfer phenomena responsible for the  $Q$  characteristics shown in Figure 18 have not been analyzed quantitatively. However, it is believed that at the higher roller bearing oil flows, some of the front bearing  $Q$  is picked up by the roller bearing oil as it flows under the front bearing. At the lower bearing oil flows this effect is diminished. In addition, at lower oil flows the roller bearing runs at higher race temperatures and conduction effects would result in heat transferred to the cooler front bearing, thus accounting for an apparent front bearing  $Q$  higher than the true value. For instance, at the lowest roller oil flow tested at 65,300 rpm, the roller bearing race temperature was about 45 degrees hotter than the front bearing race temperature. The magnitude of the roller bearing  $Q$  correction

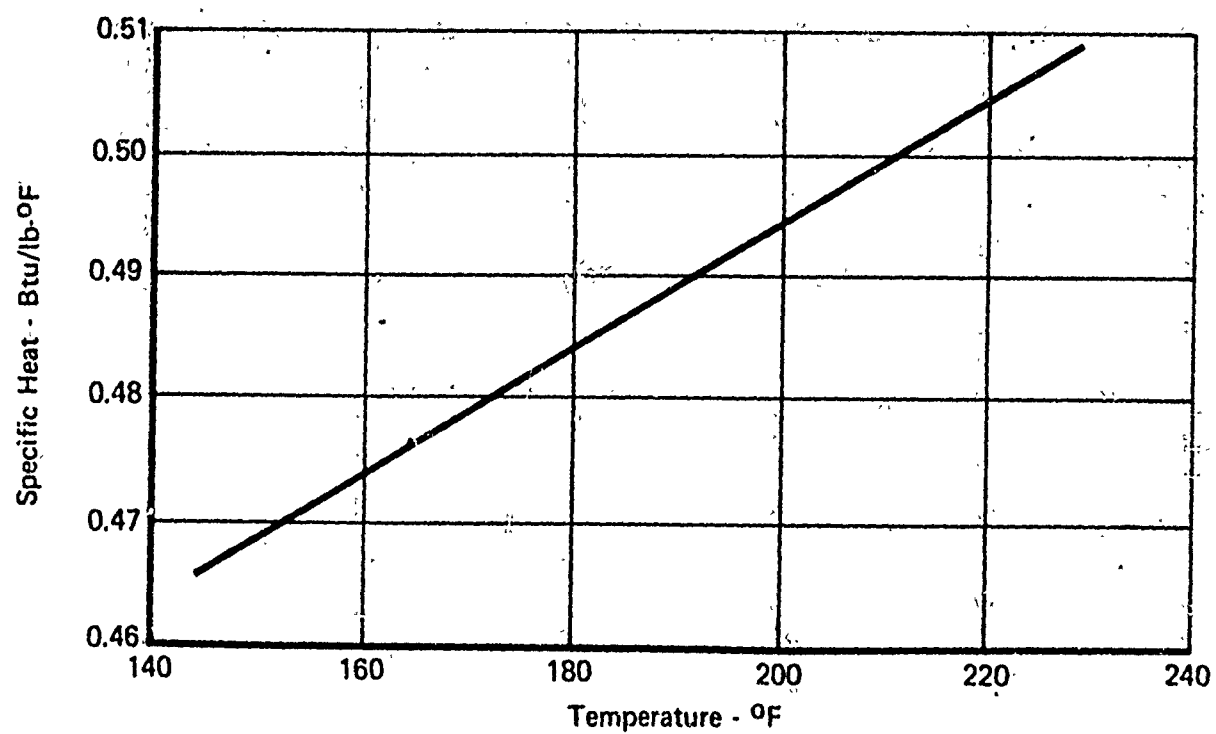
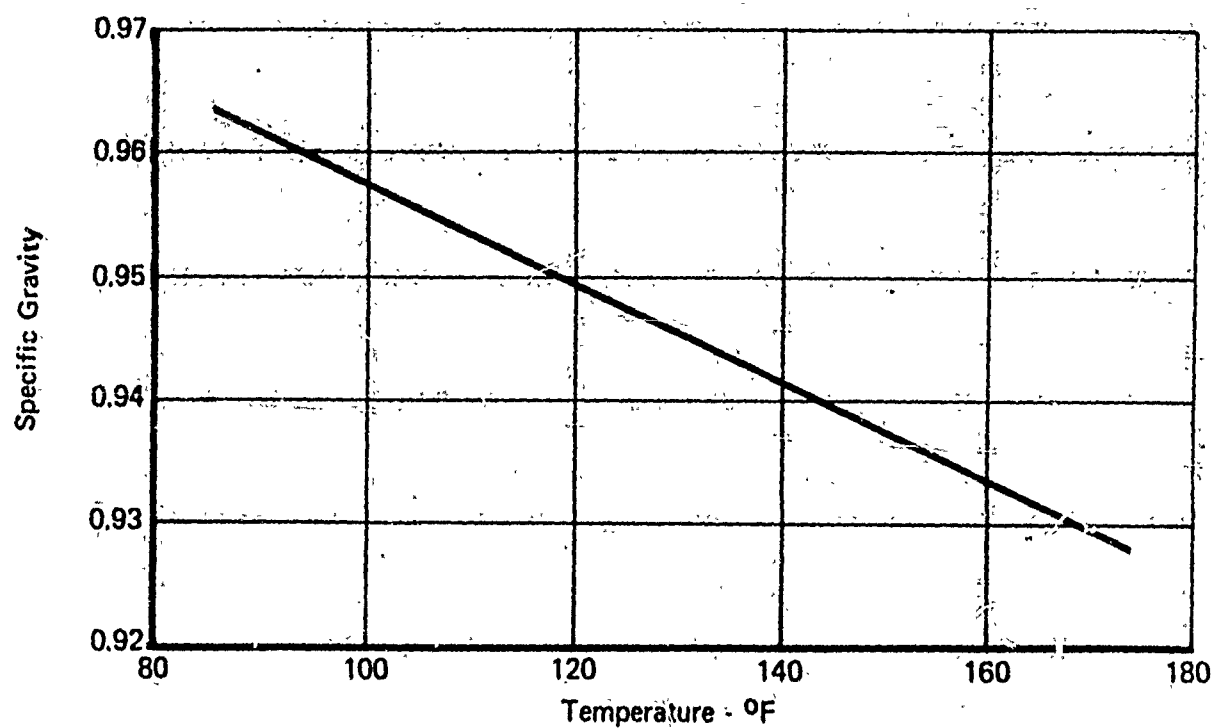


FIGURE 17 - Oil specific weight and specific heat

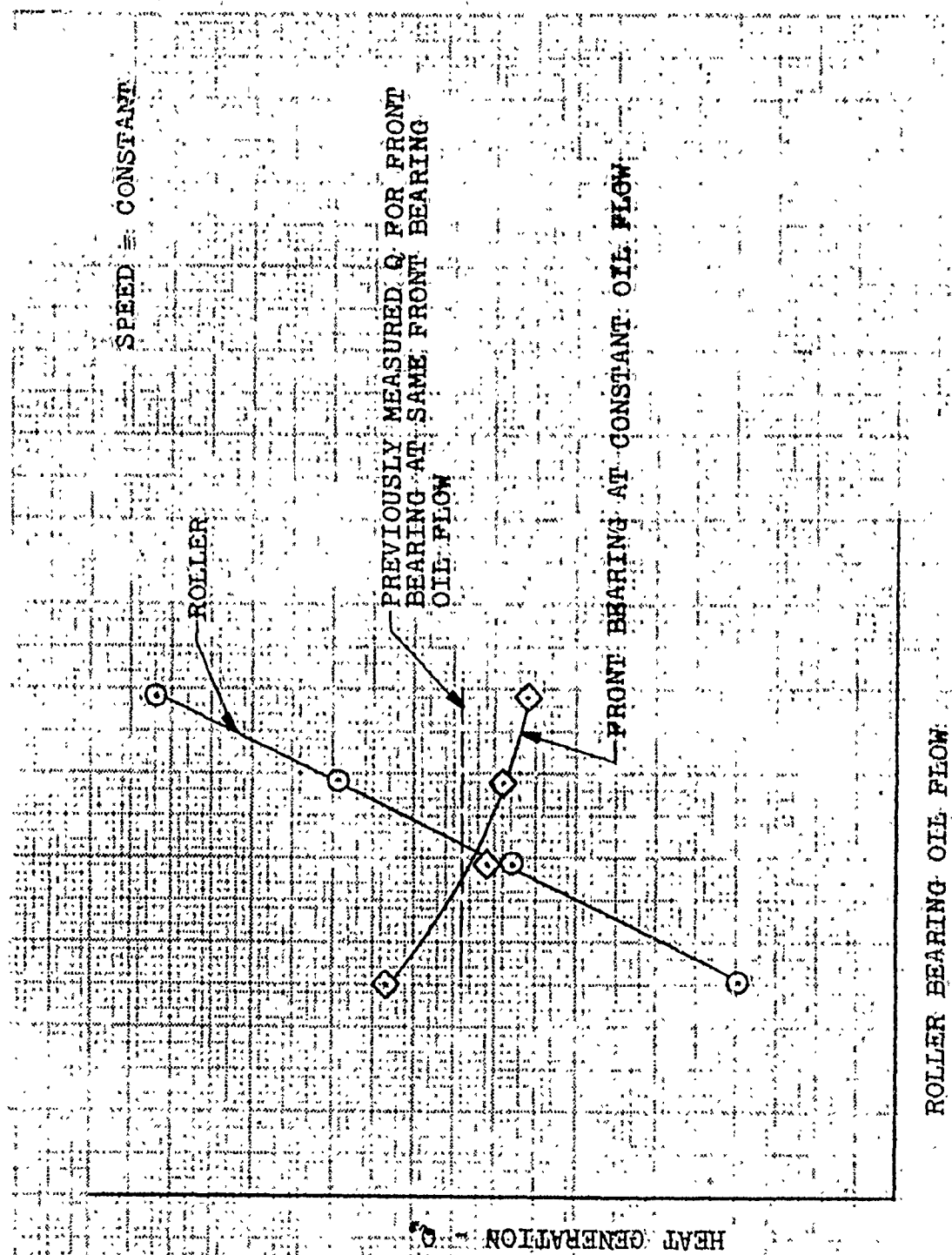


FIGURE 18 - Measured heat generation data trends

was minus 6 percent to plus 10 percent at the speed where baseline M50 data in the same oil flow range was available for comparison.

#### F. Test Results

During the entire test program, bearing rig operation was smooth and trouble-free. Vibration, temperature, and speed remained essentially constant with time at a given test condition, indicating no deterioration of any bearings.

A summary of the test data is presented in Figure 19. This table shows the as-measured parameters for the roller bearing and front ball bearing, and corrected values of heat generation for these two bearings.

The measured temperature differential between the roller bearing outer race and the oil inlet temperature is shown in Figure 20. Similar data for the oil temperature rise across the roller bearing is presented in Figure 21. Both of these curves show expected trends.

The effect of radial load on the heat generation of the roller bearing is presented in Figure 22 in both corrected and uncorrected form. Normally, it would be expected that the heat generation would show a slight increase with increased radial loads. In Figure 22, the data show a slight decrease in heat generation with an increase in load. However, the magnitude of the decrease is small (about 3.5 percent maximum), and falls within the data scatter normally experienced for this type of rig. It is concluded that the heat generation is essentially constant over the load range of 100 to 160 pounds.

The corrected heat generation of the silicon nitride roller bearing is presented in Figure 23 as a function of speed and oil flow. Although these trends are as expected, a more significant aspect of the data is how this heat generation compared with that of a similar M50 roller bearing. Such a comparison is shown in Figure 24, where M50 roller bearing corrected data<sup>13</sup> at 65,300 rpm is plotted against the silicon nitride data. These data show about 4 percent higher heat generation for the silicon nitride bearing over the oil flow range tested. One difference in the test conditions for the M50 bearing and the silicon nitride bearing is applied radial load. The M50 bearing was tested with 80 165 radial load and the silicon nitride bearing was run with 130 lbs load, which would normally result in slightly higher 'Q's for the bearing with the higher load. However, this difference would tend to be offset by the fact that the M50 bearing had a build-in "pinch" or preload, whereas the silicon nitride bearing did not. As a result, the two bearings probably had about the same radial load. Considering the normal data scatter and bearing-to-bearing differences, it is concluded that the heat generation of the silicon nitride roller bearing is comparable to that of an M50 roller bearing.

PT	#	SPEED 1000 RPM	ROLLER BEARING			FRONT BEARING (2)			CORRECTED Q <sup>3</sup>		
			LOAD LB-RADIAL	OIL FLOW LB/MIN	OIL ΔT (1) F°	OUT. RATE/OIL ΔT F°	UNCORRECTED Q BTU/MIN	OIL FLOW LB/MIN	UNCORRECTED Q BTU/MIN	FRONT BEARING (3) BTU/MIN	ROLLER BEARING BTU/MIN
1	30	130	3.9	35	39		65	5.4	71	61	75
2	30	130	2.5	36	41		43	5.5	81	62	62
3	30	130	1.1	45	51		23	5.4	88	61	50
4	45	130	3.9	63	74		119	5.4	127	115	131
5	45	130	2.5	83	71		86	5.4	122	115	93
6	45	130	1.1	81	93		43	5.6	160	117	66
7	65.3	130	5.9	98	116		284	5.3	192	208	268
8	65.3	130	4.9	99	119		239	5.3	198	208	229
9	65.3	130	3.9	102	121		196	5.3	202	208	190
10	65.3	130	2.5	112	132		139	5.4	227	212	154
11	71.5	130	5.8	110	133		316	5.4	221	242	295
12	71.5	130	4.9	112	134		273	5.3	223	240	256
13	71.5	130	3.9	116	138		225	5.2	237	237	225
14	71.5	130	2.5	128	149		159	5.2	255	237	177
15	71.5	130	2.0	129	150		135	5.5	266	245	156
16	71.5	100	3.8	119	140		227	5.3	241	240	228
17	71.5	160	3.9	116	137		225	5.4	238	242	221

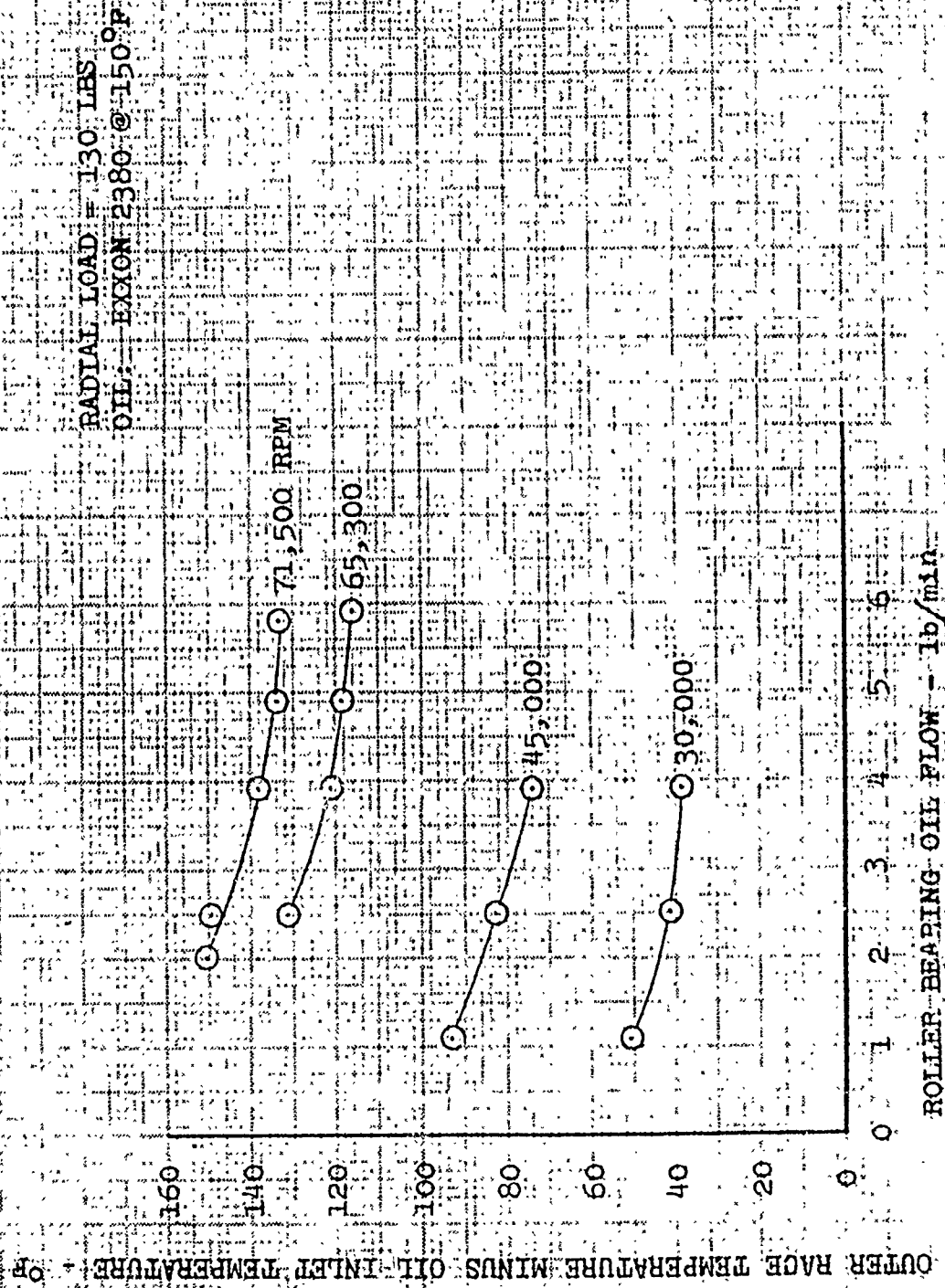


FIGURE 20 - Race/oil temperature difference (35mm Si<sub>3</sub>N<sub>4</sub> roller bearing)

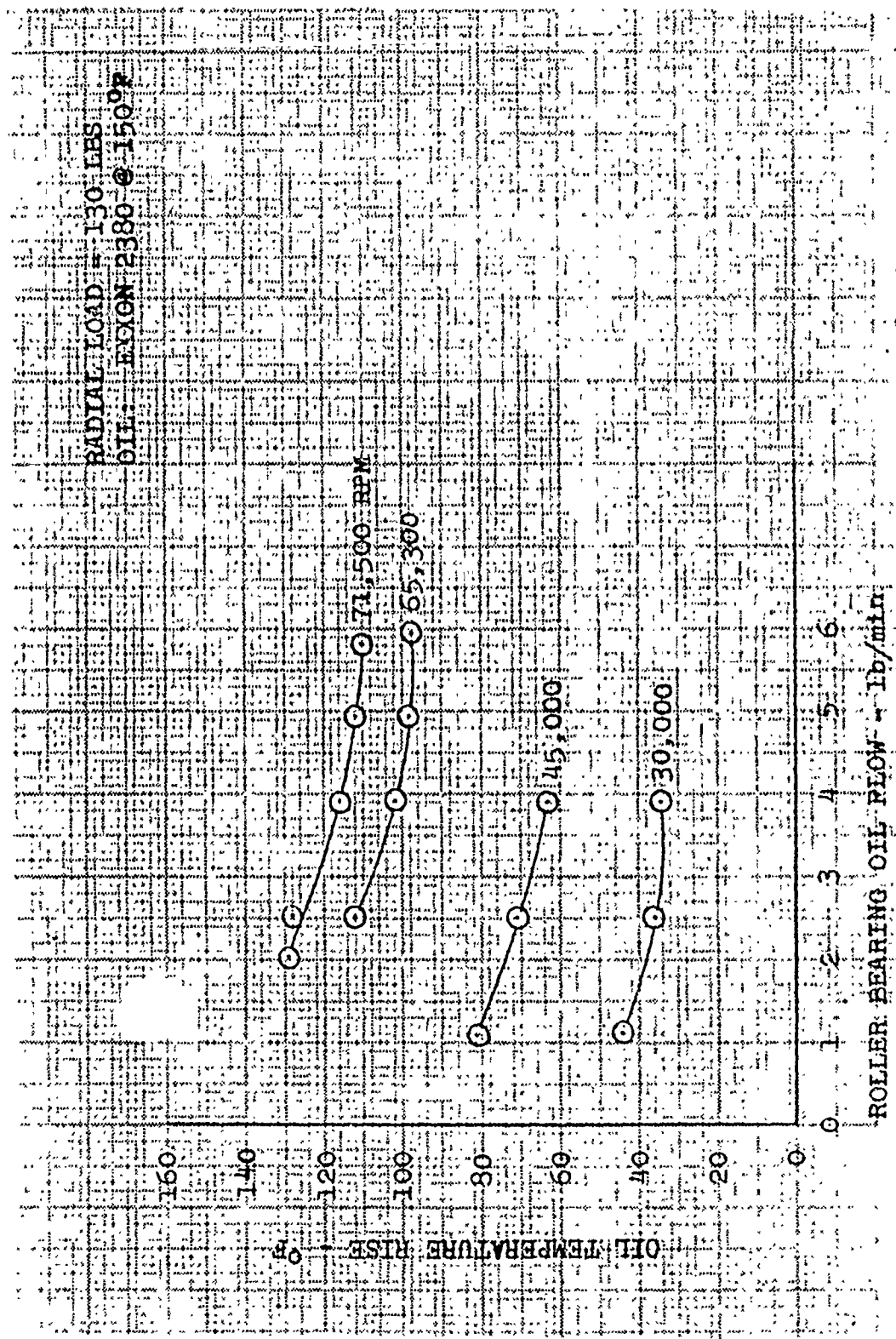


FIGURE 21 - Oil temperature rise (35mm Si<sub>3</sub>N<sub>4</sub> roller bearing)

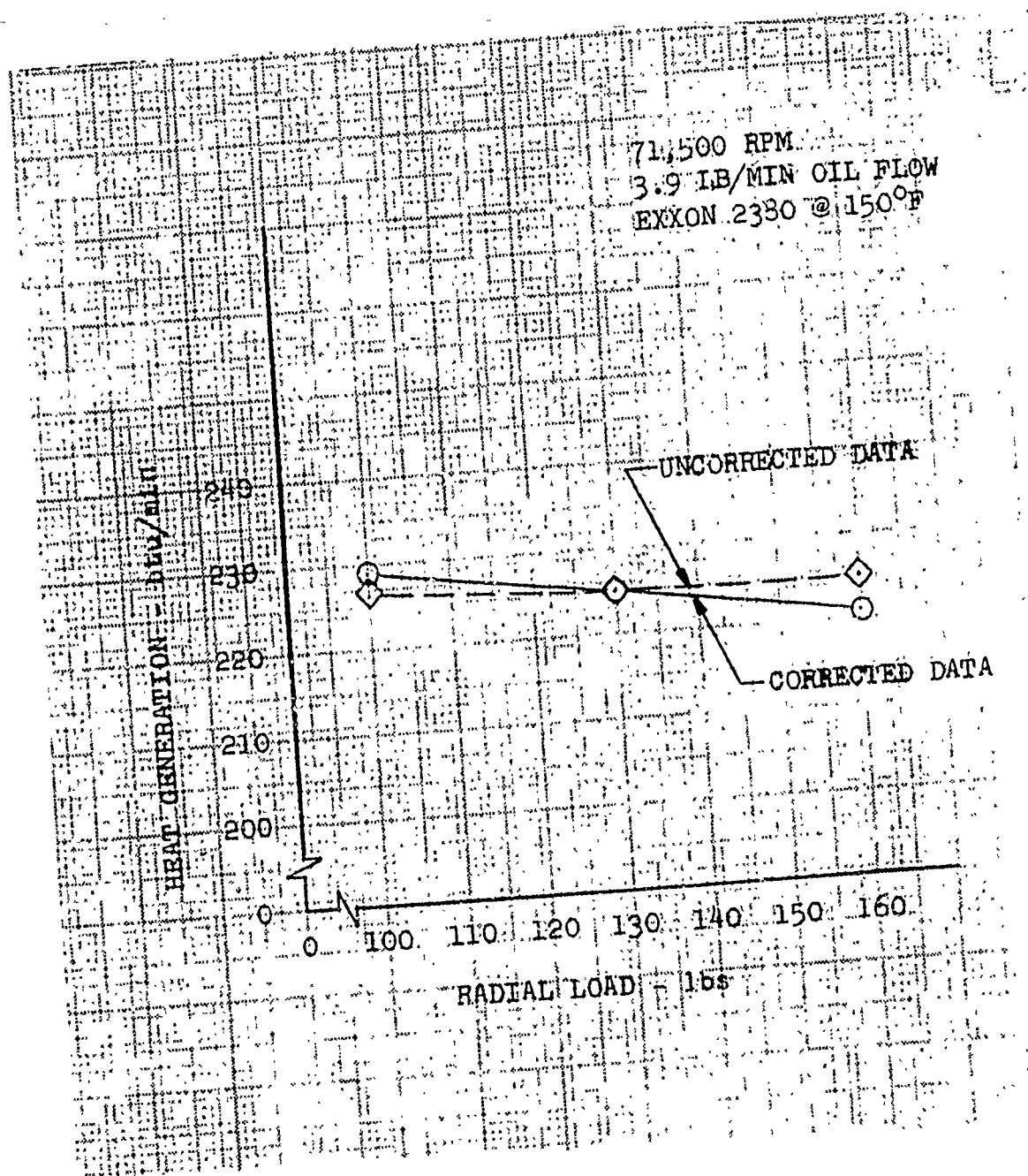


FIGURE 22 - Effect of radial load on  $\text{Si}_3\text{N}_4$  roller bearing heat generation



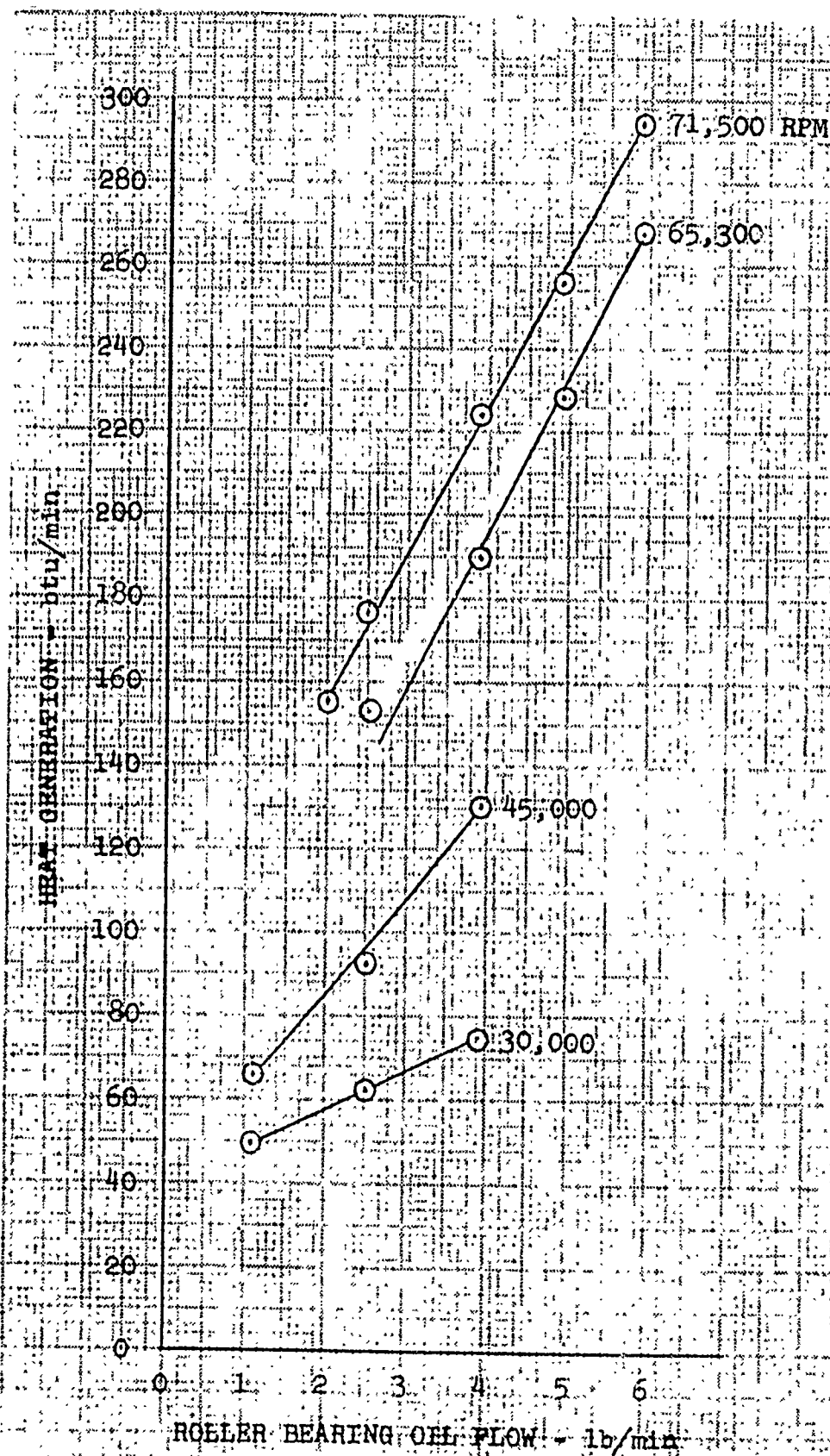


FIGURE 23 - Si<sub>3</sub>N<sub>4</sub> Roller bearing heat generation  
(Corrected for heat transfer effects)

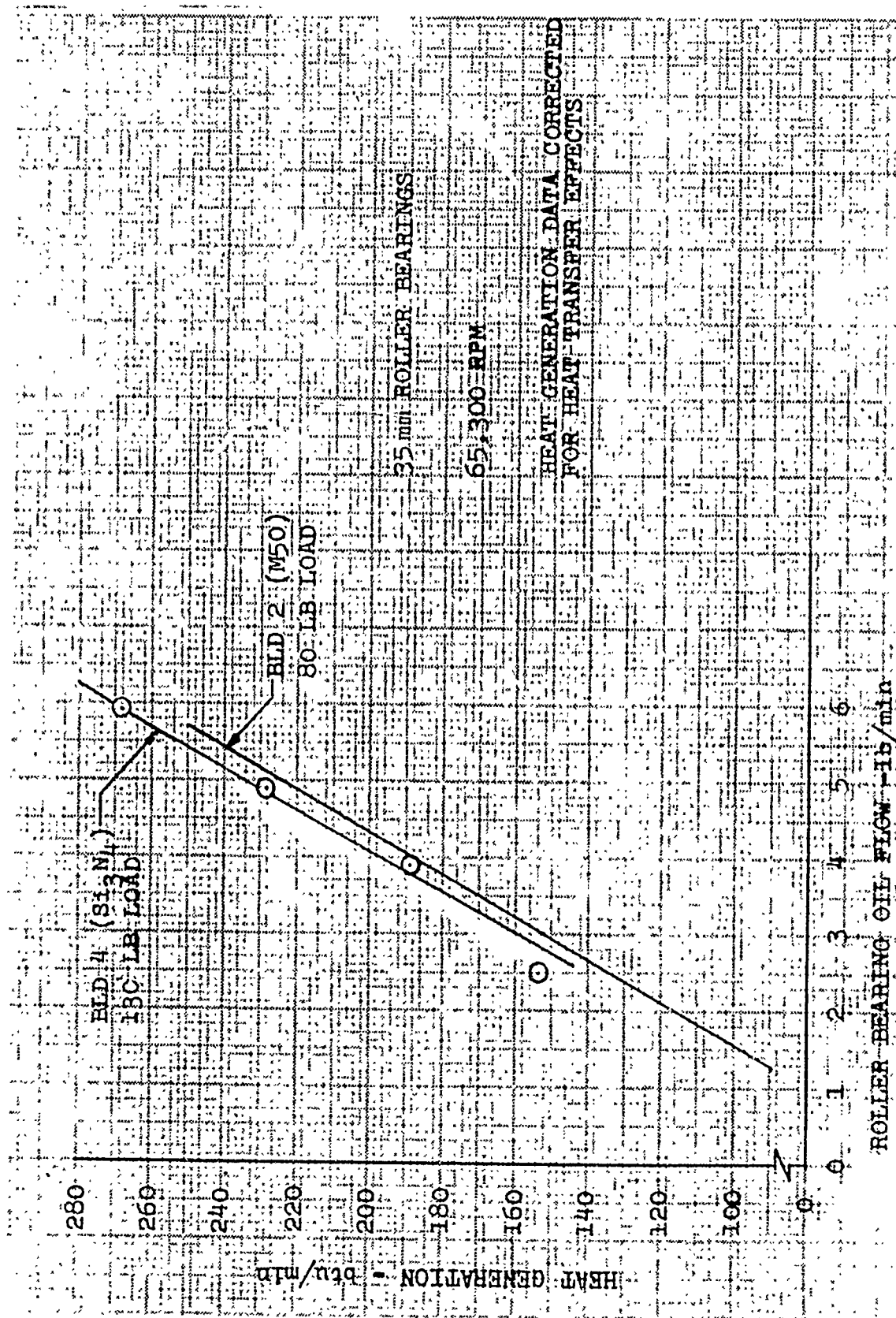


FIGURE 24 - Silicon nitride heat generation compared to M50

## VI POST TEST BEARING INSPECTION

The bearing components are shown in Figure 25 before testing and in Figure 26 after testing. Upon initial visual examination, the bearing appeared to be in good condition. However, closer examination showed that an axial crack had formed in the steel inner race surface. As will be seen, the crack was caused by a combination of a dent from a contaminate particle and the microstructure of the steel and was not related to the presence of the silicon nitride.

The crack is shown by conventional microscopy in Figure 27 and at higher magnification by scanning electron microscopy (SEM) in Figure 28. The crack extends approximately two-thirds across the raceway but does not intersect either edge. Some spalling exists at the apparent origin which is adjacent to a large contamination dent. There are several axial lines across the race and parallel to the crack. These lines are carbide segregation stringers from the steel bar stock. Inclusions of this nature are undesirable in bearing steels. The orientation of the stringers suggest that they were present in the drawn rod stock from which the races were made. The crack was probably caused by a high localized stress produced by the contamination dent and then propagated along the brittle stringer.

Another contamination dent on the inner raceway is shown in Figure 29. Three more dents were found on the outer raceway, all of similar size and shape. The indentations are approximately 0.004" wide by 0.013" long by 0.00012" deep; or, including the raised metal portions that have been worn off, they are approximately 0.007" wide by 0.015" long.

The inner race is otherwise in good condition. It has a faint running band about 0.02" wide and offset about 0.01". The offset is probably due to the offset of the roller crowns which was also about 0.01" and which was within the specification tolerance. The rollers were assembled in the bearing with their offset on the same side so as to produce the same stress per cycle condition that the races would have experienced had the crowns not been offset. Figure 30 shows axial profile traces of the raceway before and after test. There is no discernable change in the profiles. One inner race retainer guideland has circumferential scoring which was probably caused by contaminate particles trapped between the land and the cage.

The outer race is in good condition. A prominent running band, predominately straw in color with a blue center, encircles the raceway. The load zone can be readily identified from the increased width of the band from about 0.10" to about 0.14". The discoloration indicates marginally inadequate cooling. The pronounced difference in width between the inner and outer raceway running bands is caused by the centrifugal loading of the rollers

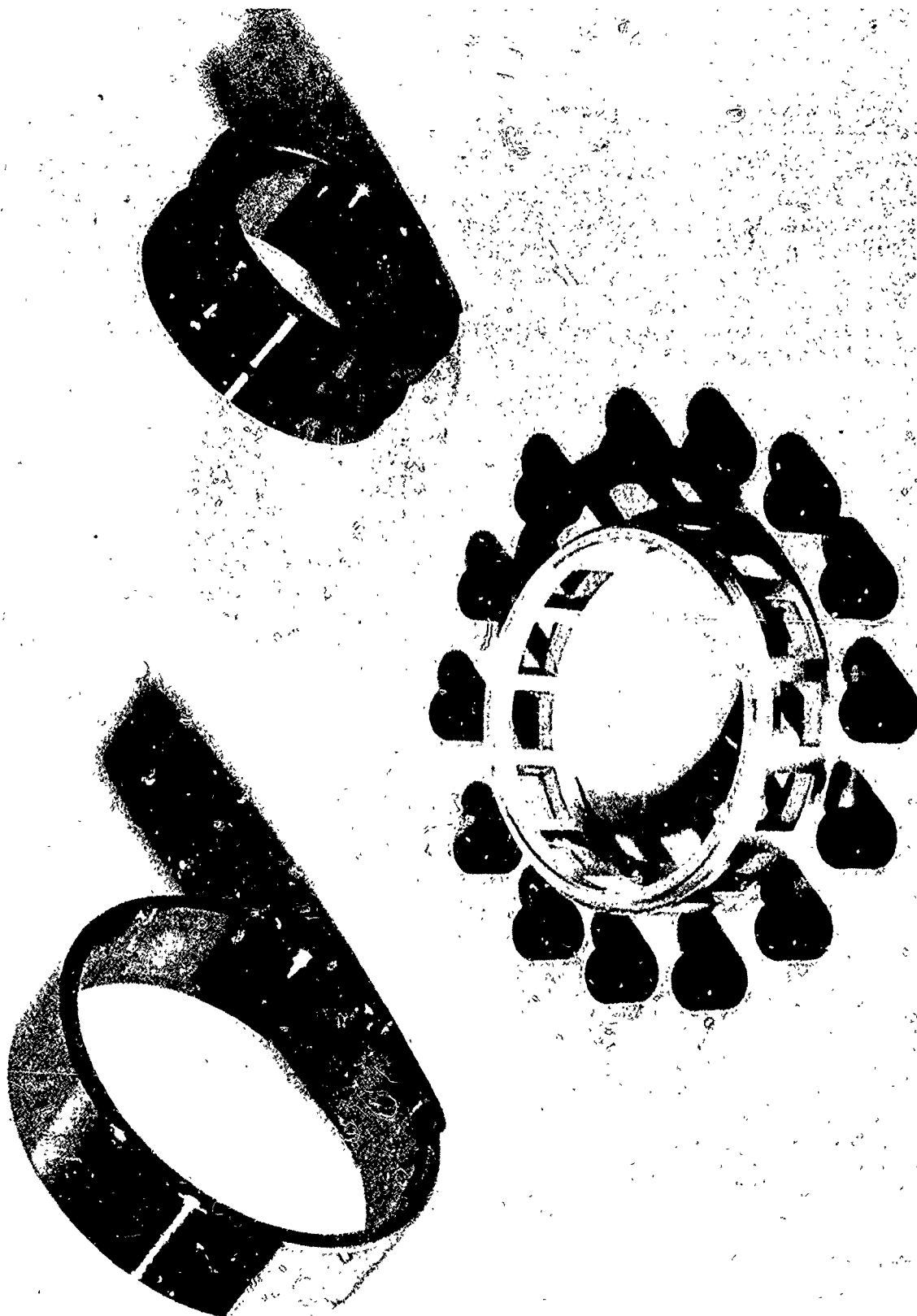


FIGURE 25 -  $\text{Si}_3\text{N}_4$  roller bearing before testing



FIGURE 26 -  $\text{Si}_3\text{N}_4$  roller bearing after testing

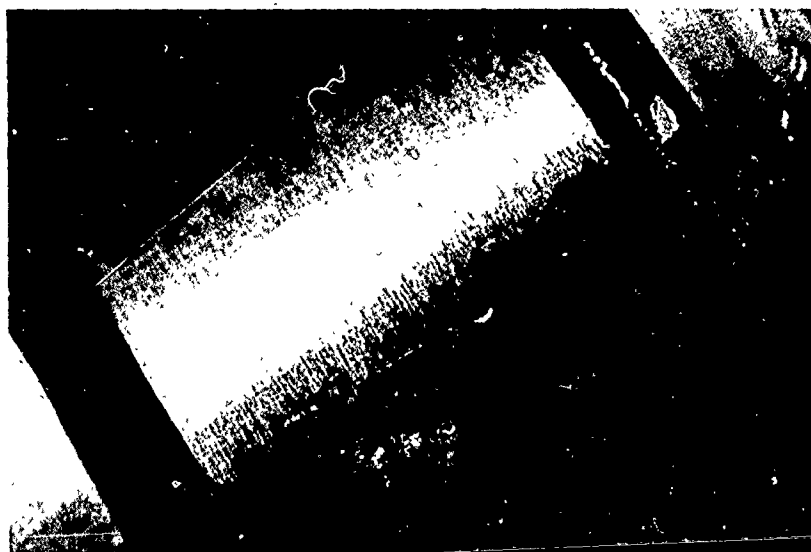


FIGURE 27 - Inner race defect, 12X

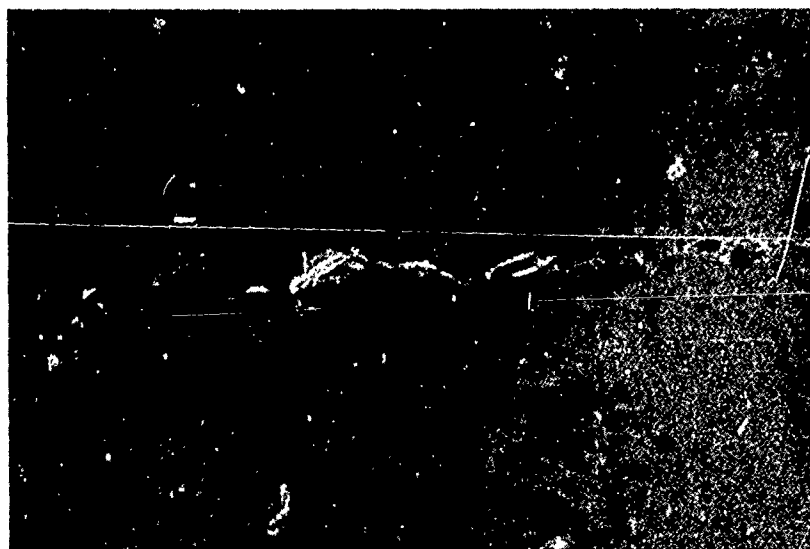


FIGURE 28 - Inner race defect, 160X, SEM



FIGURE 29 - Inner raceway dent, 12X

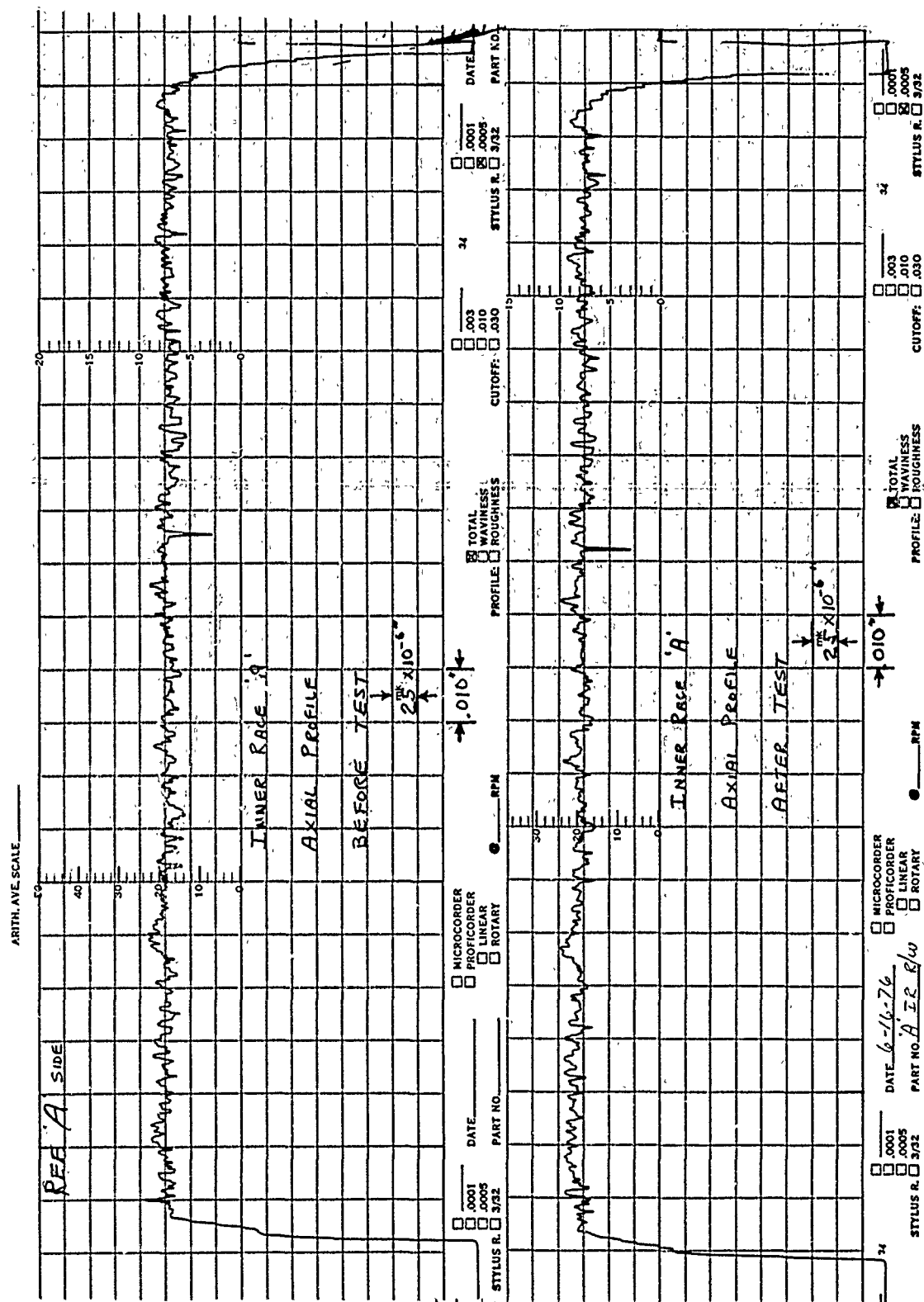


FIGURE 30 - Inner raceway axial profiles



on the outer race. There is no appreciable wear as indicated by the axial profile traces across the raceway, before and after test, shown in Figure 31.

Both raceways were free of any evidence of lubrication related surface distress. This confirms that oil quantity was always adequate for lubrication purposes and that the temperature was sufficiently low to provide adequate viscosity.

The retainer showed heavy roller contact in the pockets and a "dog-bone" wear pattern on the cross rails. "Dog-boning" is unusual for a fully crowned roller and indicates roller wobble, the cause of which is unknown, but which may have been accentuated by imbalance caused by the roller crown offset. The maximum depth of the wear on the rails is about 0.001", which is also the specified minimum silver plate thickness. Although the magnitude of the roller wobble was sufficient to wear the pockets, it did not cause any abnormal wear on the inner race roller rib walls. The walls were polished over the top one-third. The absence of abnormal wear on the rib walls is shown in the profiles, before and after test, of Figure 32. The cage cross rails showed slight discoloration, evidence of a higher than normal temperature.

Silver plated cages are used in steel bearings to prevent steel to steel sliding contact and rapid wear. For silicon nitride rollers, a different, harder pocket coating, such as molybdenum disulphide, or even no coating at all, may be beneficial.

The silicon nitride rollers were in excellent condition and show no visible sign of wear or deterioration. Roller #13 has a light circumferential score line which is probably a grinding artifact. Typical roller axial profiles, before and after test, are shown in Figure 33. Figure 34 shows high magnification photographs of roller surfaces, also before and after testing.

The radial internal clearance of the bearing assembly was measured after testing and was found to be 0.0034", the same as before the test. The inner race raceway diameter, the outer race raceway diameter, its outside diameter, and the roller diameters were all found to be unchanged (within the normal measurement scatter) by the test.

## VII CONCLUSIONS AND RECOMMENDATIONS

As a result of this program, it is concluded that:

1. It is feasible to design and fabricate roller bearings with hot-pressed silicon nitride rolling elements and conventional steel races and retainers.
2. Such a bearing can operate satisfactorily at advanced turbine engine conditions of speed, load and lubricant supply conditions.



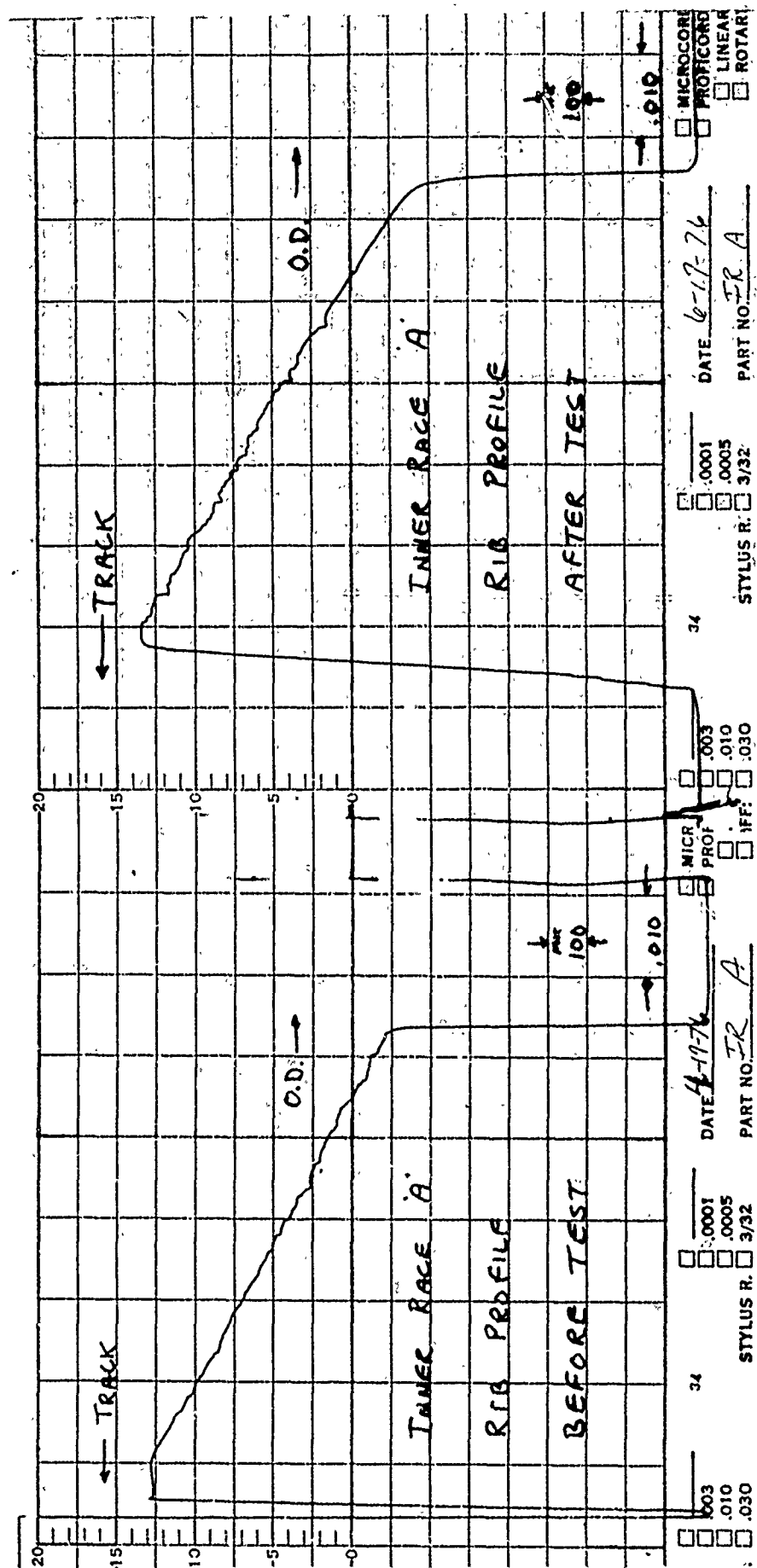


FIGURE 32 - Inner race rib wall profiles.

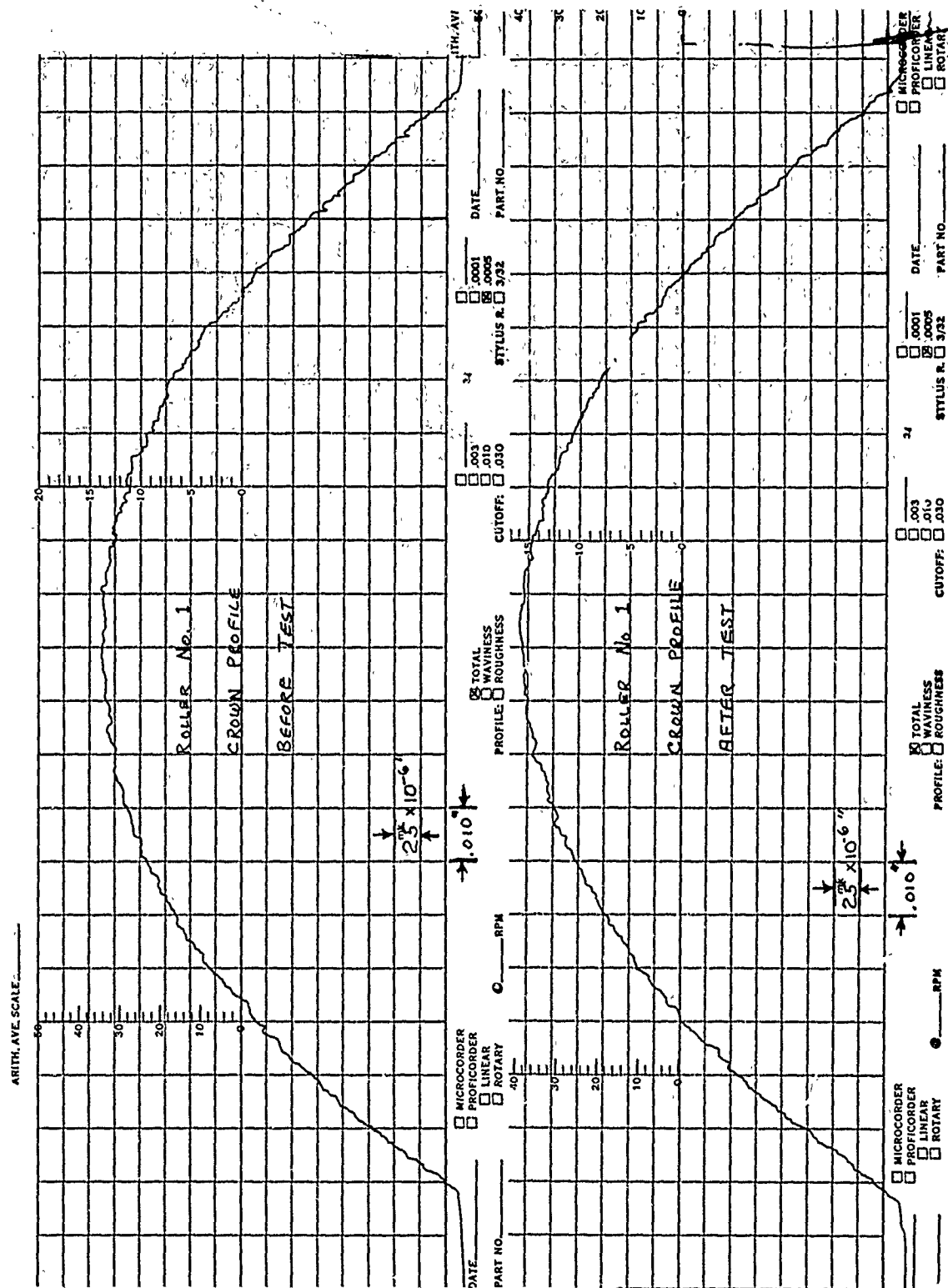
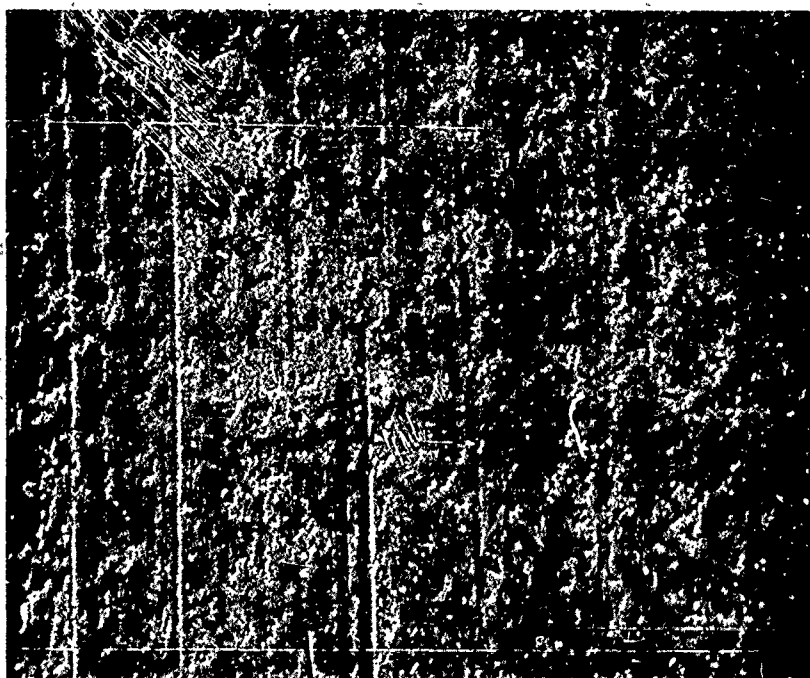
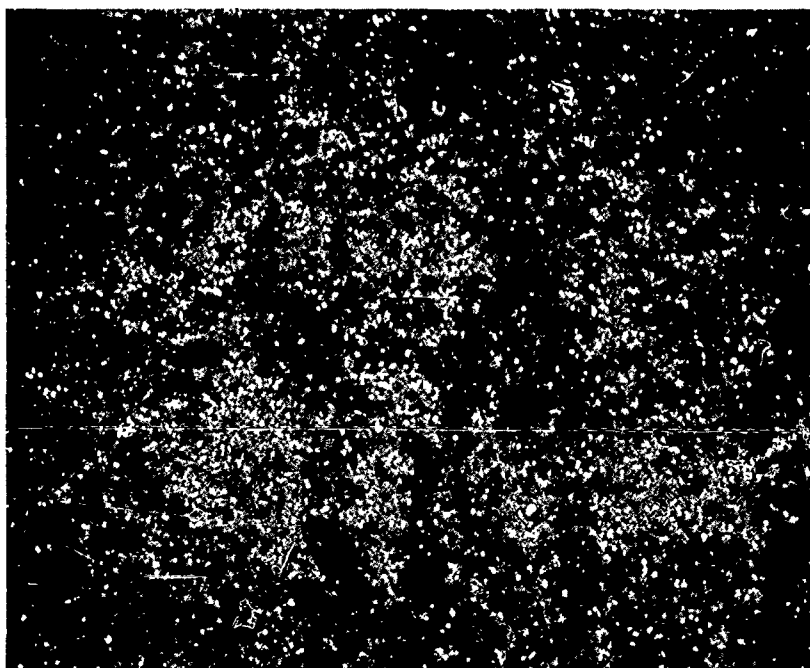


FIGURE 33 - Typical roller crown profiles



A



B

FIGURE 34 - Silicon nitride roller surface outside (A) and within (B) load zone, 500X, SEM.

3. Operating characteristics, including heat generation, of the 35mm silicon nitride roller bearing are comparable to an M50 steel bearing of the same design.

Recommendations for future work include the following:

1. Endurance tests under advanced gas turbine conditions of speed, load and lubricant should be conducted to develop additional confidence in the bearing concept.

2. A quantity of silicon nitride roller bearings should be tested to failure to develop statistically significant data for fatigue life and to define the failure mode.

## APPENDIX I

### SILICON NITRIDE CHARACTERIZATION

#### A. INTRODUCTION

The original NC-132 silicon nitride allocated for roller manufacture failed to pass the rolling contact fatigue (RCF) material qualifying procedure, although the material had been strength qualified with a mean 4-point bend strength of 133 ksi. These contrary indications of billet quality show that material strength should not be used as the sole criteria for expected bearing performance and triggered studies whose purpose it was to isolate material differences influencing rolling contact fatigue. These investigations attempted to answer two related questions: (1) What was the cause of the poor RCF performance of Billet #1? and (2) What is the effect of fracture energies on rolling contact fatigue life?

#### B. QUESTION 1

Figure A1 shows RCF lives generated at a 800 ksi contact stress on other silicon nitride billets in an attempt to identify causes of inferior fatigue behavior. Billet #1 is the rejected billet. The fatigue data were generated from specimen rods, two rods per finish variation. Finishing Method #1 is similar to the method used to prepare the roller blanks, with the exception that the final lapping was done by hand with a ring lap as opposed to a machine lap. Method #2 is the technique used to finish the RCF specimens described in the main test. The initial results were obtained with Finish #1 and indicate inferior fatigue performance. Specimens with Finish #2 were prepared to evaluate the possibility that the poor results were finishing related. Results from these specimens, although marginally better, were not sufficiently encouraging to justify the use of the billet. The thirteen tests on Billet #1 yielded an  $L_{10}$  life of about 0.16 million stress cycles, significantly inferior to lives previously obtained on silicon nitride.<sup>3,7,8,9</sup> These results formed the basis of rejecting Billet #1 for use in the program and led to an investigation of the causes of the RCF behavior.

Powder x-ray diffraction patterns were obtained from two NC-132 billets, #1 and the roller stock billet. There were no distinguishing difference between the patterns and the same phases, beta silicon nitride, silicon oxynitride and tungsten carbide were present in all.

The chemical compositions of various NC-132 billets is presented in Figure 2A. Although, minor compositional variations are evident, it is difficult to ascribe the RCF performance of Billet #1 to them. In reference nine, the chemical composition of hot-pressed silicon nitride was intentionally varied over much wider limits without producing poor RCF lives.

<u>Billet #</u>	<u>Finishing Method</u>	<u>Life (10<sup>6</sup> cycles)</u>
1*	1	0.30, 0.37, 0.92, 1.07, 1.14, 1.99, 2.85, 5.16, 8.41
1	2	0.05, 3.3, 12.6, 16.8 (suspension)
2**	2	0.10, 6.4, 8.1, 9.4
3***	2	0.07, 0.15, 4.5, 5.4

\*Rejected NC-132 Billet

\*\*NC-132 Billet

\*\*\*Billet with Intentional Calcium Addition

FIGURE A1 - RCF test results on billets of inferior fatigue life (800 ksi contact stress).

<u>Billet</u>	<u>Al</u>	<u>Ca</u>	<u>Fe</u>	<u>Mg</u>	<u>O</u>
1	0.20	0.015	0.25	0.74	1.84
4	0.38	0.04	0.58	0.46	N.M.
5	0.26	0.04	0.54	0.47	N.M.
6	N.M.	N.M.	N.M.	N.M.	1.82
7	N.M.	N.M.	N.M.	N.M.	2.21

Al, Ca, Fe, Mg determined by emission spectroscopy

O determined by gas fusion method

FIGURE A2 - Chemical analyses (w/o) of NC-132 silicon nitride billets.



The lower calcium content of the billet in question did suggest, however, a hypothesis which was subsequently evaluated. The etching of material from Billet #1 in hydrofluoric acid produced small, anomalous white spots on the surface. One of these spots is shown in Figure A3. The spot delineates a region of material which was readily attacked by the etch, leaving the more slowly etched silicon nitride crystals. Presumably, the material removed by etching is a localized concentration of the glassy bonding phase.<sup>14</sup>

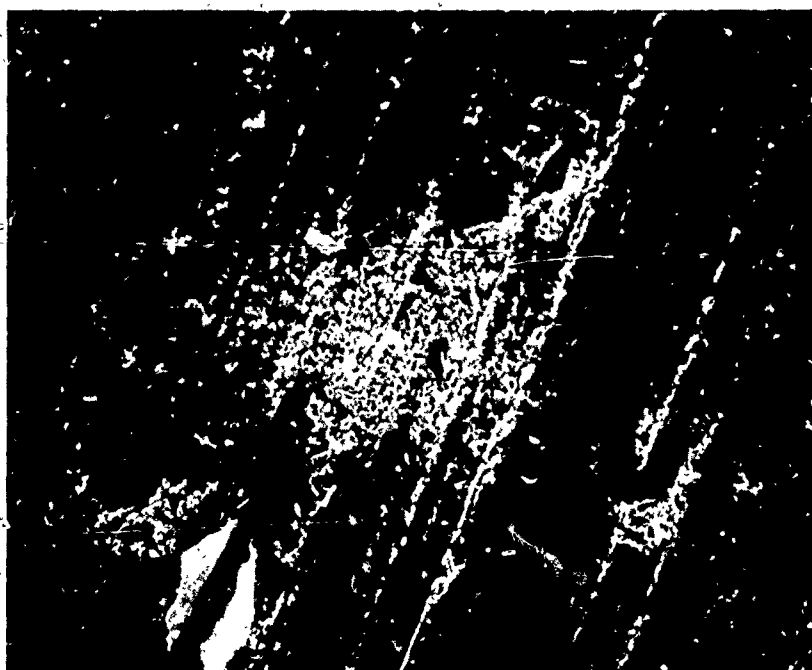
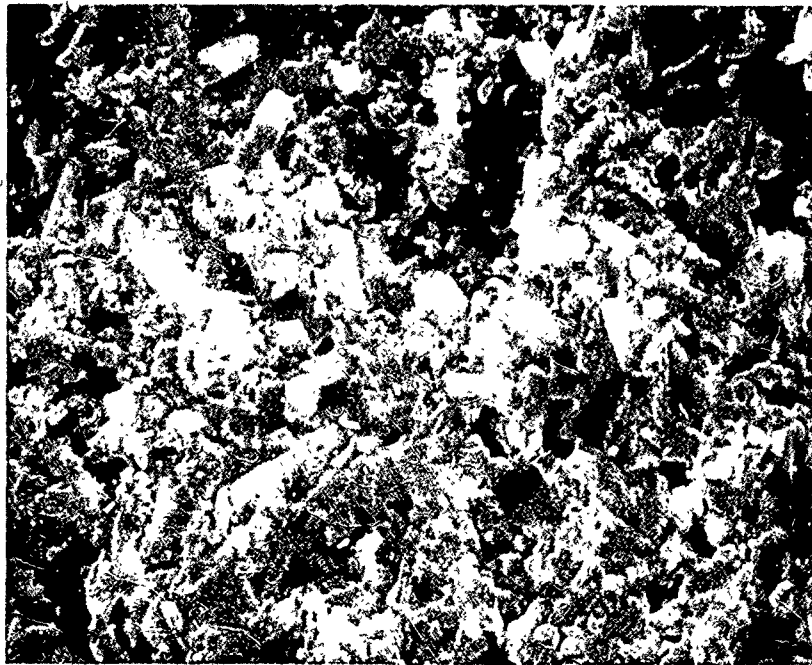


FIGURE A3 - Etch pit (white central spot) on RCF rod, 500X.

The presence of such a glass pocket in a contact load zone could cause an early fatigue spall. However, the frequency of optically visible etch pits is too small to account, by itself, for the high incidence of short fatigue lives. The presence of etch pits is, therefore, viewed as an indirect manifestation of material deficiency rather than the direct cause of the short lives. The lower calcium content of the rejected billet suggested that viscosity of the glassy bond phase may have been insufficiently low to promote complete wetting and coverage of the silicon nitride grains during hot pressing<sup>15</sup> so as to leave separate regions deficient and rich in bond phases. Even though the micrographs in Figure A4 of the two billets of differing calcium levels do not show obvious differences in bond distribution, two additional billets, one another NC-132 billet and the other containing an intentional addition of 0.03 weight percent calcium, were prepared from the



A



B

FIGURE A4 - Si<sub>3</sub>N<sub>4</sub> microstructures of material performing well (A) and poorly (B), 5000X, SEM.

same powder lot and hot pressed simultaneously, and at the same conditions used to prepare Billet #1. RCF specimens were prepared from these billets and tested. The results are included in Figure A1. It is seen that the short fatigue lives are still present and the calcium level change did not improve fatigue life.

On the basis of the above results, it must be concluded that the cause for the short fatigue lives has not been identified. The subsequent excellent fatigue lives obtained on the NC-132 silicon nitride roller stock billet from a different powder lot indicate that the difficulty may be associated with a particular powder lot.

### C. QUESTION 2

An attempt was made previously<sup>9</sup> to correlate the fracture energies of silicon nitrides differing in chemical compositions with their rolling contact fatigue lives. Fracture energies were determined by the Notched Beam Test (NBT)<sup>16</sup> and fatigue lives were measured by the RCF apparatus. Weibull L<sub>50</sub> fatigue lives were determined for each material composition by two methods. Method I included all fatigue data, while Method II disregarded very short lives which did not appear to be part of the main Weibull distribution and were a small fraction of the total number of lives. Neither method of computing the L<sub>50</sub> life correlated well with the determined fracture energies.

Dissatisfaction with this result, based upon the belief that fatigue failures and a crack propagation parameter should be related, led to a determination of the fracture energies by a second technique. Critical stress intensity factors were determined at the Naval Research Laboratory with a double cantilever beam method.<sup>17</sup>

The critical stress intensity factors were converted into fracture energies by use of the equation:

$$K_{Ic} = [2E\gamma]^{1/2}$$

where  $K_{Ic}$  = Critical stress intensity factor

E = Young's Modulus =  $45 \times 10^6$  psi

$\gamma$  = Fracture Energy

Figure A5 compiles fatigue lives and corresponding fracture energy data plus fracture energies obtained on other NC-132 silicon nitride billets. The NBT and DCB values were obtained from five and three measurements per billet, respectively.

<u>Si<sub>3</sub>N<sub>4</sub> Billet</u>	<u>γ, NBT</u> <u>J/m<sup>2</sup> ± σ</u>	<u>γ, DCB</u> <u>J/m<sup>2</sup> ± σ</u>	<u>L<sub>50</sub> Method I</u> <u>(10<sup>6</sup> cycles)</u>	<u>L<sub>50</sub> Method II</u> <u>(10<sup>6</sup> cycles)</u>
1974-3 (NC-132)	69.7 ± 1.4	(25.9 ± 8.9) *	16.7	20.0
1974-4	40.8 ± 2.5	57.5 ± 9.6	18.0	32.9
1974-5	90.7 ± 7.7	37.8 ± 9.5	31.9	31.9
1974-7	78.8 ± 12.3	62.2 ± 23.8	33.1	43.2
1974-8	87.0 ± 6.8	59.3 ± 29.8	22.0	41.6
#1 (NC-132)	47.8 ± 3.9	30.6 ± 13.0	2.0	2.0
#8 (NC-132)	N.M.	35.9 ± 19.5	N.M.	N.M.
#9 (NC-132)	N.M.	33.6 ± 32.5	N.M.	N.M.
#10 (NC-132)	N.M.	25.5 ± 16.9	N.M.	N.M.

σ = Standard Deviation                      N.M. = Not Measured

\*This reported fracture energy was measured on material from another NC-132 Si<sub>3</sub>N<sub>4</sub> billet that was hot pressed from the same powder lot, under identical conditions, on the following day.

FIGURE A5 - Silicon nitride fracture energies and fatigue lives.

The NBT and DCB methods do not rank the billets according to fracture energies in the same way for unknown reasons. However, if the DCB fracture energies are plotted against the  $L_{50}$  fatigue lives by Method II, a good correlation is obtained, as shown in Figure A6. Use of the NBT fracture energies or the  $L_{50}$  lives from Method I does not produce such a correlation. The DCB method is accepted as the more applicable method because it does supply the correlation that seems intuitively necessary. It is concluded that a high fracture energy is beneficial for superior rolling contact fatigue life.

Since Method II for computing the  $L_{50}$ 's, omits the very short lives, the correlation is further evidence that the omitted lives do belong to a separate Weibull failure branch which are not related in the same way to the fracture as is the predominant failure mode. Billet #1, the billet that was rejected for roller fabrication, does not fit the data of Figure A6 well. From Figure A5, the fracture energy of this billet is not unusual for NC-132 silicon nitride. A possible explanation for the poor fit (Figure A6) may be that the predominant failure mode in this billet is the mode that was secondary in the other billets. The lower fatigue life and the single Weibull branch for this billet support this explanation.

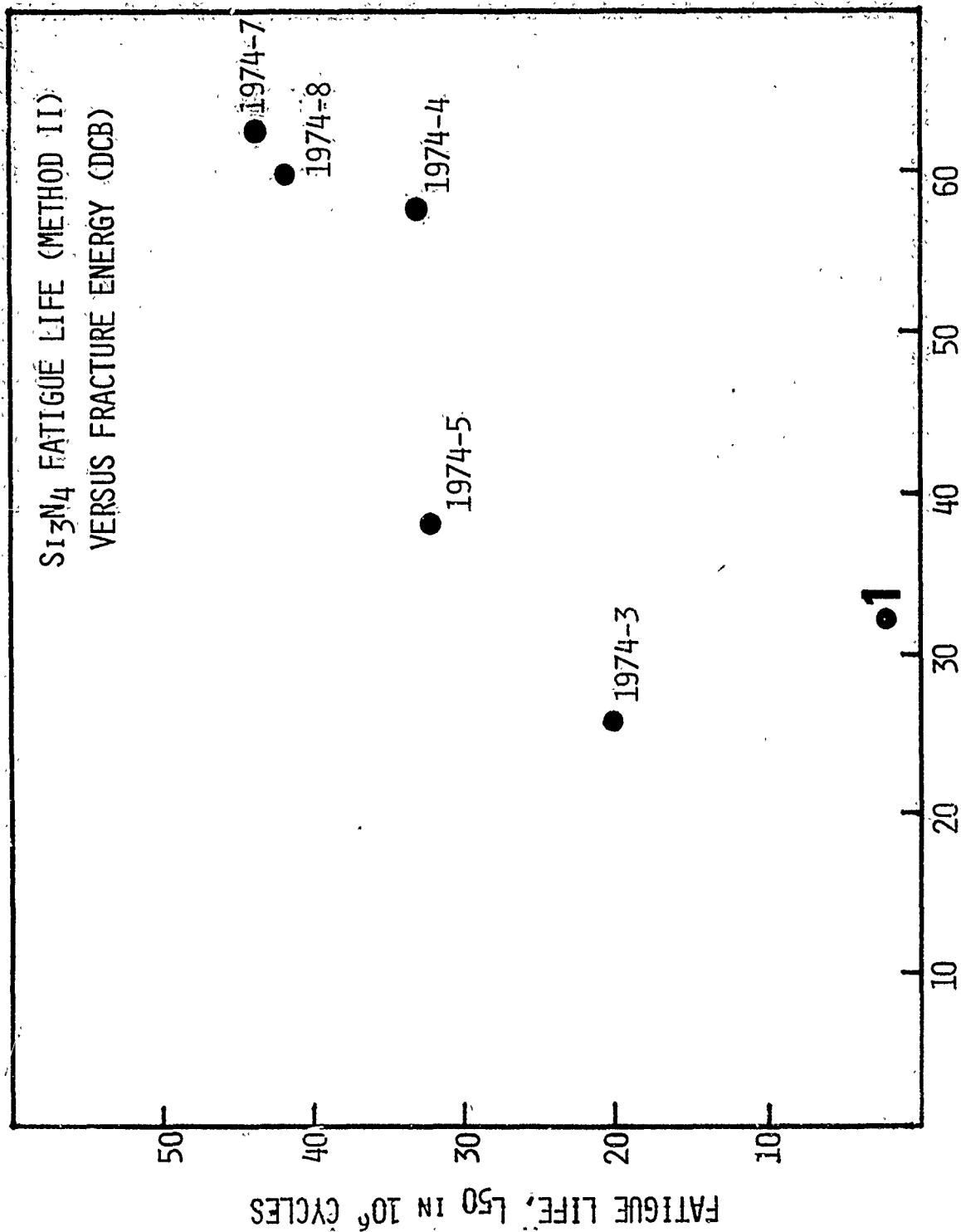


FIGURE A6 - Si<sub>3</sub>N<sub>4</sub> fatigue life (Method II versus fracture energy DCB).

## REFERENCES

1. E. V. Zaretsky and W. J. Anderson, "Rolling Contact Fatigue Studies with Four Tool Steels and Crystallized Glass Ceramic", J. Basic Eng., Trans. ASME, Series D, 83, 1961, 603.
2. R. J. Parker, S. G. Grisaffe, and E. V. Zaretsky, "Rolling Contact Studies with Four Refractory Materials to 2000°F", ASLE Trans., 8, 1965, 208.
3. W. M. Wheildon, H. R. Baumgartner, D. V. Sundberg and M. L. Torti "Ceramic Materials in Rolling Contact Bearings", Final Technical Rept under NASC Contract N00019-72-C-0299, 1973.
4. R. J. Parker and E. V. Zaretsky, "Fatigue Life of High-Speed Ball Bearings with Silicon Nitride Balls", J. Lub. Tech., Trans. ASME, Series F, 97, 1975.
5. R. Valori, "Rolling Contact Fatigue of Silicon Nitride", Naval Air Propulsion Test Center Report NAPTC-PE-42, 1974.
6. H. Dalal, "Surface Interactions and Lubrication Response of Silicon Nitride Bearing Elements", Final Report under NASC Contract N00019-73-C-0193, 1973.
7. H. R. Baumgartner and P. E. Cowley, "Finishing Techniques for Silicon Nitride Bearings", Final Report under Army Materials and Mechanics Research Center Contract DAAG46-74-C-0055, 1976.
8. H. R. Baumgartner, D. V. Sundberg, and W. M. Wheildon, "Silicon Nitride in Rolling Contact Bearings", Final Report Under NASC Contract N00019-73-C-0193.
9. H. R. Baumgartner and P. E. Cowley "Silicon Nitride in Rolling Contact Bearings", Final Report under NASC Contract N00019-74-C-0157, 1975.
10. J. M. Reddecliff and R. Valori, "The Performance of a High-Speed Ball Thrust Bearing Using Silicon Nitride Balls, Paper No. 76-LubS-8 presented at the ASME Lubrication Symposium, Atlanta, GA., May 24-26, 1976.
11. J. J. Petrovic, L. A. Jacobson, P. K. Talty and A. K. Vasudevan, "Controlled Surface Flaws in Hot-Pressed  $\text{Si}_3\text{N}_4$ ", J. Am. Ceram. Soc., 58, 1975, 113.
12. Reference 8, page 12.
13. Previously unpublished, Pratt and Whitney Aircraft.

14. S. Wild, P. Grieverson, K. H. Jack, M. J. Latimer, "Role of Magnesia in Hot-Pressed Silicon Nitride", in Special Ceramics 5, P. Popper, ed., Brit. Ceram. Res. Assoc. 1972, 377.
15. R. Kossowsky, "Wetting of Silicon Nitride by Alkaline-doped  $\text{MgSiO}_3$ ", J. Matls. Sci., 9, 1974, 2025.
16. S. D. Hartline, R. C. Bradt, H. R. Baumgartner and N. B. Rosebrooks, "Notched-Beam Test for Fracture-Energy Measurement", J. Am. Ceram. Soc. 56, 1973, 550.
17. S. W. Freiman, D. R. Mulville and P. W. Mast, "Crack Propagation Studies in Brittle Materials", NRL Report 7575, July 1973.



# DISTRIBUTION LIST FOR CONTRACT N00019-75-C-0197

AIR-52032, Naval Air Systems Command Washington, D.C. 20360	4
Naval Air Systems Command Washington, D.C. 20360 Attention: AIR 604	10
Office of Naval Research Washington, D.C. 20360 Attention: Code 471	1
Naval Ordnance Laboratory White Oak, Maryland 20910 Attention: Code 2301	1
Ceramic Finishing Company Box 498 State College, PA 16801	1
Materials Sciences & Engineering Laboratory Stanford Research Institute Menlo Park, CA 84025	1
Inorganic Materials Division Institute for Materials Research National Bureau of Standards Washington, D.C. 20234	1
Battelle Memorial Institute 505 King Avenue Columbus, OH 43201	1
Metals and Ceramics Information Center Battelle Memorial Institute 505 King Avenue Columbus, OH 43201	1
IIT Research Institute 10 West 35th St Chicago, Illinois 60616 Attention: Ceramics Division	1
Naval Air Propulsion Test Center Trenton, NJ 08628 Attention: R. Valori	1
Materials Application Branch Aero Materials Laboratory (VTD) Naval Air Development Center Warminster, PA 18974	1

Naval Ship R&D Laboratory 1  
Annapolis, Maryland 21402  
Attention: Watt Smith (Code 2832)

Naval Ship Research and Development Center 1  
Washington, D.C. 20007  
Attention: K. Nishida

Naval Undersea R&D Center 1  
San Diego, CA 92117  
Attention: Dr. J. Stachiw

Air Force Materials Laboratory 5  
Wright-Patterson Air Force Base  
Dayton OH 45433  
Attention: LMD 1  
LAE 1  
LAM 1  
LT 1  
LNL 1

Naval Research Laboratory 2  
Washington, D.C. 20390  
Attention: Code 6360 1  
Code 8430 1

NASA Headquarters 1  
Washington, D.C. 20546  
Attention: J.J. Gangler, RRM

Lewis Research Center 2  
21000 Brookpark Road  
Cleveland, OH 44135  
Attention: Dr. E. Zaretsky 1  
W. A. Sanders (49-1) 1

Materials Research Center 1  
Lehigh University  
Bethlehem, PA 18015  
Attention: Dr. D. P. H. Hasselman

Department of Metallurgy 1  
Case-Western Reserve University  
Cleveland, OH 44106  
Attention: Dr. A. Heuer

Westinghouse Research Labs. 1  
Beulah Road  
Churchill Borough  
Pittsburgh, PA 15235  
Attention: Dr. R. Bratton

Dept. of Engineering Research  
North Carolina State University  
Raleigh, NC 27607  
Attention: Dr. H. Palmour

1

Battelle Memorial Institute  
Pacific Northwest Laboratory  
Richland, Washington 99352  
Attention: P. L. Farnsworth

1

Materials Engineering Department  
University of Rhode Island  
Kingston, RI 02881  
Attention: Dr. Peter Gielisse

1

Turbine Research Department  
Product Development Group  
Ford Motor Company  
20000 Rotunda Drive  
Dearborn, MI 28121

1

Aerospace Corporation  
Materials Laboratory  
P.O. Box 95085  
Los Angeles, CA 90045  
Attention: Dr. R. C. Rossi

1

U. S. Army Research Office  
Box CM, Duke Station  
Durham, NC 27706  
Attention: CRDARD

1

Ceramic Division  
Sandia Corporation  
Albuquerque, NM 87101

1

Applied Technology Division  
Avco Corporation  
Lowell Industrial Park  
Lowell, MA 01851

1

Solar Division  
International Harvester Company  
2200 Pacific Highway  
San Diego, CA 92112  
Attention: Dr. A. G. Metcalfe

1

Midwest Research Institute  
425 Volker Boulevard  
Kansas City, Missouri 64110  
Attention: G. Gross

1

Bell Aerosystems Company Buffalo, NY 14240 Attention: Materials Research & Structural Systems Department	1
Materials Sciences Laboratory United Aircraft Corporation East Hartford, CT 06101	1
Metallurgy and Ceramics Research Dept General Electric R&D Laboratories P.O. Box 8 Schenectady, NY 12301	1
Engineering Experiment Station Georgia Institute of Technology Atlanta, Georgia 30332 Attention: J. D. Walton	1
Materials Research Laboratory Pennsylvania State University University Park, PA 16802 Attention: Prof. Rustum Roy	1
National Beryllia Corporation Greenwood Avenue Hasket, NJ 07420	1
Hughes Aircraft Company Aerospace Group R&D Division Culver City, CA 90130	1 1
Space Sciences Laboratory General Electric Company P.O. Box 8555 Philadelphia, PA 19101	1
Department of Engineering University of California Los Angeles, CA 90024 Attention: Profs. J. W. Knapp and G. Sines	1
North American Rockwell Science Center P. O. Box 1085 Thousand Oaks, CA 91360	1
Library, Stellite Division Cabot Corporation 1020 W. Park Avenue Kokomo, Indiana 46901	1

Marlin-Rockwell Division  
TRW Inc.  
Jamestown, NY 14701  
Attention: A. S. Irwin

1

The Boeing Company  
Materials and Processes Labs  
Aerospace Group  
P.O. Box 3999  
Seattle, Washington 98124

1

Research Department  
Ampex Corporation  
401 Broadway  
Redwood City, CA 94063

1

Army Materials and Mechanics  
Research Center  
Watertown, MA 02172  
Attention: Dr. R. N. Katz

1

Coors Porcelain Company  
600 Ninth Street  
Golden, Colorado 80401  
Attention: Research Department

1

Federal-Mogul Corporation  
Anti-Friction Bearing R&D Center  
3980 Research Park Drive  
Ann Arbor, Michigan 48104  
Attention: D. Glover

2

Industrial Tectonics Inc.  
18301 South Santa Fe  
Compton, CA 90224  
Attention: H. Hanau

1

Pratt & Whitney Aircraft Division  
United Aircraft Corporation  
Florida R&D Center  
West Palm Beach, Florida  
Attention: Glen Calvert

1

Southwest Research Institute  
P.O. Drawer 28510  
San Antonio, Texas 78228

1

Fiber Materials, Inc.  
Broadway and Main Streets  
Graniteville, MA 01829

1

Pratt & Whitney Aircraft Division United Aircraft Corporation East Hartford CT 06108 Attention: Paul Brown EB-2	1
Engineering and Research Center SKF Industries, Inc. 1100 First Avenue King of Prussia, PA 19406	1
School of Ceramics Rutgers, The State University New Brunswick, NJ 08903	1
Union Carbide Corporation Parma Technical Center P.O. Box 6116 Cleveland, Ohio 44101	1
Research and Development Division Carborundum Company Niagara Falls, NY 14302	1
U. S. Army MERDC Fort Belvoir, VA 22060 Attention: W. McGovern (SMEFB-EP)	1
Supervisor, Materials Engineering Dept 93-39M AirResearch Mfg Co of Arizona 402 South 36th Street Phoenix AZ 85034	1
Ferro Corporation Technical Center 7500 East Pleasant Valley Road Independence, Ohio 44131	1
Air Force Aero Propulsion Laboratory Wright-Patterson Air Force Base, Ohio 45433 Attention: Ron Dayton (SFL)	1
Research and Development Division Arthur D. Little Company Acorn Park Cambridge, MA 02140	1
Detroit Diesel Allison Division General Motors Corporation P. O. Box 894 Indianapolis, Indiana 46206 Attention: Dr. M. Herman	1

Mechanical Technology, Inc.  
968 Albany-Shaker Road  
Latham, NY 12110  
Attention: Dr. E. F. Finkin

1

Aircraft Engine Group  
Technical Information Center  
Main Drop N-32, Bldg 700  
General Electric Company  
Cincinnati, Ohio 45215

1

Astronuclear Laboratory  
Westinghouse Electric Corporation  
Box 10864  
Pittsburgh, PA 15236

1

Caterpillar Tractor Company  
Technical Center  
East Peoria, Illinois 61611  
Attention: A. R. Canady

1

Curtiss-Wright Company  
Wright Aeronautical Division  
One Passaic Street  
Wood-Ridge, New Jersey 07075

1

Fafnir Bearing Company  
Division Textron Corporation  
27 Booth Street  
New Britain, CT 06050

1

Lycoming Division  
Avco Corporation  
Stratford, CT 06497

1

Pratt and Whitney Aircraft Division  
United Aircraft Corporation  
Middletown, CT 06108  
Attention: L. E. Friedrich, MERL

1

Rollway Bearing Company  
Division Lipe Corporation  
7600 Morgan Road  
Liverpool, NY 13088  
Attention: B. Dalton

1

NDH Division  
General Motors Corporation  
Hayes Street  
Sandusky, Ohio  
Attention: H. Woerhle

1

Teledyne CAE  
1330 Laskey Road  
Toledo, Ohio 43601  
Attention: R. Beck 1

The Timken Company  
Canton, Ohio 1  
Attention: R. Cornish  
Williams Research Corporation 1  
Walled Lake, Michigan 48088

Marlin Rockwell, Division of TRW  
Jamestown, NY 14701 1  
Attention: John C. Lawrence

Industrial Tectonics, Inc.  
18301 Santa Fe Avenue 1  
Compton, CA 90224  
Attention: Hans R. Signer

F.A.G. Bearing Corporation  
70 Hamilton Avenue 1  
Stamford, CT 06904  
Attention: Joseph Hoo

University of California  
Lawrence Berkeley Laboratory 1  
Hearst Mining Building  
Berkeley, CA 94720  
Attention: Dr. L. Roschauer

Naval Air Systems Command  
AIR 310C 1  
Washington, DC 20361  
Attention: Dr. H. Rosenwasser

Naval Air Systems Command  
AIR 536 1  
Washington DC 20361

Naval Air Systems Command  
AIR 330 1  
Washington DC 20361



UNCLASSIFIED

Security Classification

## DOCUMENT CONTROL DATA - R &amp; D

(Security classification of title, body of abstract and indexing annotation must be entered when the overall report is classified)

1. ORIGINATING ACTIVITY (Corporate author) Norton Company, Industrial Ceramics Division One New Bond Street Worcester, Massachusetts 01606		2a. REPORT SECURITY CLASSIFICATION	
		2b. GROUP	
3. REPORT TITLE <u>CERAMIC MATERIALS IN ROLLING CONTACT BEARINGS.</u>			
4. DESCRIPTIVE NOTES (Type of report and inclusive dates) Final (15 March 1975 to 15 September 1976)			
5. AUTHOR (Last name, middle initial, first name) H. Robert Baumgartner Glen S. Calvert Paul E. Cowley		9. Final rept. 15 Mar 75-15 Sep 76	
6. REPORT DATE 11 Oct 76		7c. TOTAL NO. OF PAGES 63	7d. NO. OF FIGURES 41 Figures
8a. CONTRACT OR GRANT NO. N00019-75-C-0197 NEW		8b. ORIGINATOR'S REPORT NUMBER(S) 12 63p.	
c.		8d. OTHER REPORT NUMBER (Any other numbers that may be assigned this report)	
d.			

10. DISTRIBUTION STATEMENT APPROVED FOR PUBLIC RELEASE; DISTRIBUTION UNLIMITED	
11. SUPPLEMENTARY NOTES	12. SPONSORING MILITARY ACTIVITY Department of the Navy Naval Air Systems Command Washington, DC 20360

13. ABSTRACT  
The objectives of the program were to design, fabricate and evaluate the performance of a roller bearing having hot-pressed silicon nitride rollers and steel races at speeds up to 71,500 rpm (2.5 million DN). The 35mm bore bearing consists of AISI-CVM M50 steel races, fourteen fully crowned NC-132 silicon nitride rollers and a silver plated AMS 6414 steel retainer.

Bearing performance was defined in terms of operating temperature, heat generation and vibration at speeds between 30,000 and 71,500 rpm under a predominately 130 pound radial load. Following the calibration testing, the bearing was endurance tested an additional 19 hours at 71,500 rpm.

The bearing test operation was smooth and trouble-free. Heat generation of the silicon nitride roller bearing was comparable to that of a similar M50 steel roller bearing.

Post-test bearing inspection showed the bearing to be in generally good condition with the major exception of a crack in the inner steel raceway that was caused by the interaction of a contamination dent and a carbide inclusion. Some roller wobble had occurred, as indicated by retainer pocket wear.

UNCLASSIFIED

Security Classification

14 KEY WORDS	LINK A		LINK B		LINK C	
	ROLE	WT	ROLE	WT	ROLE	WT
Ceramic Silicon Nitride ( $\text{Si}_3\text{N}_4$ ) Wear High Strength Materials Rolling Contact Fatigue (RCF) Surface Preparation Ceramic Bearings Roller Bearings High Speed Bearings						

UNCLASSIFIED